CHARACTERIZING SELECTIN-LIGAND BONDS USING ATOMIC FORCE MICROSCOPY (AFM)

A Thesis
Presented to
The Academic Faculty

By

Krishna Kumar Sarangapani

In Partial Fulfillment
of the Requirements for the Degree
Doctor of Philosophy in Bioengineering

Georgia Institute of Technology
August 2005

CHARACTERIZING SELECTIN-LIGAND BONDS USING ATOMIC FORCE MICROSCOPY (AFM)

Approved by:

Dr. Cheng Zhu, Advisor
School of Biomedical Engineering and
Department of Mechanical Engineering
Georgia Institute of Technology

Dr. Donald P. Giddens
School of Biomedical Engineering
Georgia Institute of Technology

Dr. Rodger P. McEver
Cardiovascular Biology Research Program
Oklahoma Medical Research Foundation

Dr. Dr. Shuming Nie
School of Biomedical Engineering
Georgia Institute of Technology & Emory University

Dr. Mei-Yin Chou
School of Physics
Georgia Institute of Technology

Date Approved: May 02, 2005

ACKNOWLEDGMENTS

At the outset, I would like to thank my advisor Dr. Cheng Zhu. Without his guidance and help, I would not be penning down this section. Like any other student, I have been through good and bad times in my PhD stint and my advisor stood by me all the time, goading me to set high standards and excel every time. Thanks to him, I truly feel I have become a good researcher. Second of all, I would like to thank Dr. Rodger McEver, who has been an outstanding mentor and research collaborator. Besides graciously providing almost all the reagents that I have worked with, he helped me critically analyze bioengineering problems from a biological perspective and as a result, I started relating basic engineering and biological principles with relative ease. I would also like to thank my other committee members Drs. Giddens, Nie and Chou for their guidance and support.

My karmic connection with the AFM was firmly established when I started working with Dr. Bryan Marshall. He taught me all the tricks of the trade and was patient enough to answer all my questions. As the saying goes 'Well begun is half done'. I couldn't have asked for a better start than being trained initially by him. Tim Tolentino was one other person who really put me at ease, when I first stepped into the Zhu lab. He taught me all the basics in the most lucid way and for this, I am indebted to him. Besides, there were and are many other fellow members in the Zhu lab who have been really kind and helpful to me all through and made my everyday life at the Zhu lab, a pleasant experience.

My stay here at Georgia Tech wouldn't have been so wonderful had it not been for my amazing circle of friends. They have stood by me through thick and thin and helped me in my professional as well as personal development.

I would like to thank my parents and my brother and his family for supporting me all along. I very vividly remember my brother telling me that I should keep trying hard and should always settle for nothing but the best. I sincerely hope I have lived up to my kith and kin's expectations.

Finally, I would like to thank my dear Swami, Bhagawan Sri Sathya Sai Baba for providing me this wonderful opportunity of doing a PhD at a very good institution. When I think of it, I feel that he has been there all along - guiding, guarding and protecting me and helping me achieve my goals. It would seem like an understatement if I profusely thank Him but I feel I am duty-bound to say it anyways: Thank You, Swami!

TABLE OF CONTENTS

LIST OF FIGURES

LIST OF ABBREVIATIONS

AFM: Atomic Force Microscopy

(s)PSGL-1: (Soluble) P-selectin Glycoprotein Ligand 1

ESL-1: E-selectin Ligand 1

2-GSP-6: 2 Glycosulfopeptide 6

2-GP-1: 2 Glycopeptide 1

6-Sulfo-sLe^{x}: 6 Sulfo Sialyl Lewis X

mAb: monoclonal antibody

CR: Consensus Repeat

ICAM: Intercellular Cell Adhesion Molecule

VCAM: Vascular Cell Adhesion Molecule

MAdCAM: Mucosal Addressin Cell Adhesion Molecule

PECAM: Platelet and Endothelial Cell Adhesion Molecule

NCAM: Neural Cell Adhesion Molecule

BSA: Bovine Serum Albumin

HBSS: Hanks Balanced Salt Solution

DPBS: Dulbeccos Phosphate Buffered Saline

EDTA: Ethylene Diamine Tetraacetate

HEV: High Endothelial Venules

CHO: Chinese Hamster Ovary

cDNA: Complementary DNA

DFS: Dynamic Force Spectroscopy

MPRF: Most Probable Rupture Force

pN: picoNewton

nm: nanometer

STD: Standard Deviation

S.E.M: Standard Error of Measurements

SUMMARY

The human body is an intricate network of many highly regulated biochemical processes and cell adhesion is one of them. Cell adhesion is mediated by specific interactions between molecules on apposing cell surfaces and is critical to many physiological and pathological processes like inflammation and cancer metastasis. During inflammation, blood-borne circulating leukocytes regularly stick to and roll on the vessel walls, which consist in part, adhesive contacts mediated by the selectin family of adhesion receptors (P-, E- and L-selectin). This is the beginning of a multi-step cascade that ultimately leads to leukocyte recruitment in areas of injury or infection.

In vivo, selectin-mediated interactions take place in a hydrodynamic milieu and hence, it becomes imperative to study these interactions under very similar conditions *in vitro*. The goal of this project was to characterize the kinetic and mechanical properties of selectin interactions with different physiologically relevant ligands and selectin-specific monoclonal antibodies (mAbs) under a mechanically stressful milieu, using atomic force microscopy (AFM).

Elasticity studies revealed that bulk of the complex compliance came from the selectins, with the ligands or mAbs acting as relatively stiffer components in the stretch experiments. Furthermore, molecular elasticity was inversely related to selectin length with the Consensus Repeats (CRs) behaving as Hookean springs in series. Besides, monomeric vs. dimeric interactions could be clearly distinguished from the elasticity measurements. L-selectin dissociation studies with P-selectin Glycoprotein Ligand 1 (PSGL-1) and Endoglycan revealed that catch bonds operated at low forces while slip

bonds were observed at higher forces. These results were consistent with previous P-selectin studies and suggested that catch bonds could contribute to the shear threshold for L-selectin-mediated rolling By contrast, only slip bonds were observed for L-selectin-antibody interactions, suggesting that catch bonds could be a common characteristic of selectin-ligand interactions. Force History studies revealed that off-rates of L-selectin-sPSGL-1 (or 2-GSP-6) interactions were not just dependent on applied force, as has been widely accepted but in fact, depended on the entire history of force application, thus providing a new paradigm for how force could regulate bio-molecular interactions.

Characterizing selectin-ligand interactions at the molecular level, devoid of cellular contributions, is essential in understanding the role played by molecular properties in leukocyte adhesion kinetics. In this aspect, data obtained from this project will not only add to the existing body of knowledge but also provide new insights into mechanisms by which selectins initiate leukocyte adhesion in shear.

CHAPTER 1

INTRODUCTION AND SPECIFIC AIMS

The human body is an intricate network of highly regulated biochemical processes and cell adhesion is one of them. Cell adhesion is mediated by specific interactions between cell adhesion molecules (CAMs) and is critical to many physiological and pathological processes, including tissue choreography during organ formation, inflammation and cancer metastasis. Inflammation is the human body's natural and immediate response to an injury or an infection (when an intruder organism manages to compromise the outer skin barrier and enters the body). What follows is a series of highly regulated processes that are aimed at removing the anomaly and restoring equilibrium. During an inflammatory response, white blood cells (WBCs) or leukocytes and macrophages that act as the sentinels of the defense system are directed towards the affected areas.

Leukocyte extravasation to sites of tissue injury or infection involves a cascade of mechanisms, the initial phase of which includes selectins. Either induced on activated endothelial cells (P- and E-selectin) or expressed constitutively on leukocyte surfaces (L-selectin), their rapid transient interactions with ligands such PSGL-1 mediate the tethering and rolling of leukocytes on vascular surfaces prior to firm adhesion and diapedisis (McEver 1991). Each selectin has an affinity for oligosaccharides with Sialyl Lewis x (sLe^x) or Sialyl Lewis a (sLe^a) determinants. Selectin-mediated cell adhesion is based on carbohydrate recognition of Calcium-dependent Lectin. PSGL-1 is a physiologically relevant ligand for all the selectins and is perhaps the best biochemically

characterized. It is a mucin-like carbohydrate presenting molecule with two 120 kD subunits which are disulfide-linked (McEver and Cummings 1997).

OVERALL OBJECTIVE AND SPECIFIC AIMS

Selectin-ligand adhesive bonds link cells in a hydrodynamic milieu and, it is necessary to characterize these interactions under very similar conditions *in vitro*. Also, characterizing selectin-ligand interactions at the molecular level devoid of cellular contributions is essential to understand the role played by molecular properties in leukocyte adhesion kinetics. The goal of this research was to characterize the interactions of P-, E- and L-selectin with different ligands (and mAbs) under mechanically stressful environments. Atomic force microscopy (AFM) was used to extract the kinetic and mechanical properties of the selectin-ligand (or –mAb) bonds. The approach and retraction of the AFM cantilever tip decorated with ligands (or mAbs) into and away from a selectin-incorporated lipid bilayer mimicked the process of a leukocyte approaching to and departing from the endothelia. Three specific aims were designed in order to address some questions concerning the selectins.

SPECIFIC AIM #1: DELINEATING THE MECHANICAL PROPERTIES OF SELECTIN-LIGAND COMPLEXES

Selectin-ligand bonds form and break under the auspices of the flowing blood and under this mechanically stressful milieu, their mechanical properties could be pertinent to their physiological function. However, very little is known about such properties. Previous studies have employed AFM to probe the mechanical features of

macromolecules like titin (Kellermayer et al. 1997; Rief et al. 1997). These studies involved stretching the molecules with very high forces and characteristic saw-tooth *Force vs. Molecular Extension* behavior was observed. These studies elegantly demonstrated the unfolding and refolding patterns of the individual protein domains and modeled the systems using appropriate models. Fritz et al. have reported the elasticities of P-selectin-PSGL-1 complex but there are some obvious concerns about this work. For example, in this study, biotinylated P-selectin-Ig and PSGL-1-Ig chimeras were used (where the antibody alone on average was modified with 10 biotins) to immobilize the molecules on the coverslips and on the AFM tips (Fritz et al. 1998). This could have most likely resulted in random lengths of the specimens that were stretched. Also, the presence of a zero-force molecular extension (dead zone) gave the appearance of a nonlinear *Force vs. Molecular Extension* relationship. This might have prompted the use of the modified free joint chain (MFJC) model, which depicted P-selectin and PSGL-1 as chain-like polymers that required little initial force to straighten their randomly coiled shapes (Fritz et al., 1998). Both the invalid model and the poor experimental protocol may have contributed the inaccurate P-selectin spring constant of 5.3 ± 1.5 pN/nm (Fritz et al. 1998). By comparison, we used bilayer and capture protocols for immobilizing the selectins and ligands to ensure uniform lengths of the molecular complexes being stretched.

To date, no comprehensive results about the mechanical properties of the selectins have been published. It is logical to surmise that understanding the mechanical features of the selectins could shed some light on why selectin-ligand bonds are efficient in linking cells under mechanically stressful conditions. With this idea in mind, the *Force vs.*

Molecular Extension behaviors and elasticities of various selectin-ligand (or mAb) complexes were characterized. Specifically, the relative contributions of the selectins as well as the ligands (or mAbs) to the complex compliance were looked at. The idea of using a mechanical property like elasticity to identify key biochemical features (like *monomeric vs. dimeric interactions* mediated by the different selectins) was novel in this study.

SPECIFIC AIM #2: DISSECTING THE BOND LIFETIME-FORCE RELATIONSHIP OF L-SELECTIN INTERACTIONS WITH PSGL-1, sPSGL-1, ENDOGLYCAN AND DREG56

Bell proposed that force could accelerate bond dissociation by lowering the energy barrier between bound and free states (Bell 1978). Conversely, Dembo et al. envisioned a finger-prison model in which applied force could lock the bond tighter, thereby decelerating bond dissociation (Dembo et al. 1988). These two types of bonds are called slip and catch bonds respectively. While many studies reported slip bonds, counter-intuitive catch bonds were demonstrated only recently in P-selectin-mediated interactions (Marshall et al. 2003). PSGL-1 is a homodimeric mucin on leukocyte surface (McEver and Cummings 1997). P- and L-selectin interact with PSGL-1 in a related manner, suggesting that like P-selectin, L-selectin could also form catch bonds with PSGL-1. Hence, the interactions of L-selectin with two forms of PSGL-1: a wild-type dimeric form (PSGL-1) and a soluble monomeric form (sPSGL-1) were examined. Furthermore, Endoglycan, a newly identified PSGL-1-like ligand of the CD34 family of

sialomucins was also tested (Fieger et al. 2003). L-selectin interactions with an anti-L-selectin mAb, DREG56, were used as a system control.

SPECIFIC AIM #3: CHARACTERIZING THE FORCE HISTORY DEPENDENCE OF L-SELECTIN-LIGAND DISSOCIATION

Off-rates can be extracted by employing the theory of Dynamic Force Spectroscopy (DFS) that analyzes the *Most Probable Rupture Force (MPRF) vs. Rate of Force Application* curve based on an assumed relationship between off-rate and force (Evans and Ritchie 1997). Previous P-selectin studies have revealed that off-rates measured directly from bond lifetimes and from DFS analysis of unbinding forces differed drastically, suggesting that the off-rate was not just a single-valued function of force but depended on the entire history of force application (Marshall et al. 2005). It was not known whether this concept was true for other selectins as well or P-selectin-mediated interactions were an isolated example system. Hence, additional validation was required to confirm the force history concept. To further test this unconventional idea in a simplified manner, specific AFM experiments were designed and performed to measure L-selectin-sPSGL-1 (and -2GSP-6) bond lifetimes at a given force reached via different paths. As a system control, L-selectin interactions with a sulfated sugar (6-sulfo-sLe^x) were also characterized.

CHAPTER 2

BACKGROUND

2.1 Cell Adhesion and Cell Adhesion Molecules (CAMs)

The capability of cells to recognize and adhere to each other and to the secreted macromolecules that constitute the extracellular matrix (ECM) is one of the basic requirements for the existence of multicellular organisms. The adhesive linkages between the cells enable them to form cooperative assemblies called tissues, which again associate to form larger functional units, the organs. Eukaryotic cells adhere to other cells or the ECM in order to maintain the architecture of specific organs. The ability of cells to recognize and specifically adhere to other cells or the ECM is very critical to many physiological and pathological processes as well. Examples include homing of lymphocytes to specific lymphoid organs, margination of leukocytes at sites of inflammation and injury and metastatic spread of tumor cells (Springer 1990; McEver 1991).

Frequently, cells make switches between adherent and non-adherent states in a highly controlled and regulated fashion. For instance, during inflammation, white blood cells circulating through the body roll on and stick to vessel endothelia in post-capillary venules. Lymphocytes regularly stick to the endothelia in the High Endothelial venules (HEV), migrate into the tissues for sampling of processed antigens, and exit through the lymphatics. During hemorrhage, platelets stick to exposed subendothelial matrix components, spread and recruit additional platelets into large aggregates that serve as an efficient surface for thrombin and fibrin generation, thus plugging the vessel rupture.

Predominantly, cells adhere through non-covalent bonds formed between macromolecules on their surfaces with macromolecules on apposing surfaces (which could be another cell or ECM). These molecules are termed cell adhesion molecules (CAMs). These interactions involve either protein-protein or protein-carbohydrate recognition.

Receptors are protein molecules that are involved in signaling. They possess an extracellular domain for binding ligands (e.g. growth factors, adhesion molecules etc) and an intracellular or cytoplasmic domain. They may or may not possess a transmembrane domain (for example, GPI-anchored proteins). Receptor-driven cell behavior plays an extremely important role in growth, secretion, contraction, motility, and adhesion. Receptors, by virtue of their ability to sense the environment, are able to direct cell behavior through binding of ligands, and their ability to transmit this signal to the cell interior, through interaction of their intracellular domains with enzymes and proteins within the cell. Many adhesion molecules can be grouped into families according to related structural and functional features. To date, receptors belonging to at least four major super-families have been identified: Integrins, Immunoglobulins, Cadherins and Selectins.

INTEGRINS

Integrins are a broadly distributed group of cell-surface adhesion receptors with non-covalently associated α- and β-subunits. Several different α- and β-subunits are known to date, which are expressed in various, but not all of the possible combinations on the surface of most cell types and are involved in many cell-cell and cell-matrix

interactions (Springer 1990). Both integrin subunits are necessary for surface expression and ligand binding. The β_2 integrins, paired with a unique α- subunit are also called leukocyte integrins because they are found only on leukocyte surfaces. GPIIb/IIIa is expressed only by megakaryocytes and platelets. In many cases, integrins have been shown to bind to proteins containing the tripeptide sequence arginine-glycine-aspartate (RGD).

The cytoplasmic domain of integrins is relatively short (~ 50 amino acids) but it has been shown to have a very important function in conveying information from the outside into the cell interior (outside-in signaling) as well as conveying information from the cell interior to the outside (inside-out signaling). Hence, integrins are transmembrane proteins that are known to interact simultaneously with both extracellular ligands and cytoskeletal components. For example, in the case of the integrin Leukocyte Function-Associated Antigen 1 (LFA-1), signals from the cytosol are transduced across the membrane to generate changes in extracellular functions such as adhesion. Further, affinity modulation of the integrins to their ligands helps the cell control its adhesiveness to a substrate or to another cell (Shimaoka 2000).

IMMUNOGLOBULIN-LIKE RECEPTORS

The immunoglobulin super-family members contain a variable number of disulfide-stabilized β-barrel domains that are linked to transmembrane and cytoplasmic domains. The immunoglobulin-like domain provides a framework to which specific recognition structures for other proteins can be added. Immunoglobulins, T-cell receptor, and Class I & Class II MHC molecules, all of which are involved in immune reactions

belong to this super-family (Springer 1990). These members of the family possess variable regions resulting in affinity maturation due to somatic hypermutation. Typical examples include the Immunoglobulins (IgG, IgA etc), the Intercellular Adhesion Molecules (ICAM-1, ICAM-2 etc) and the Vascular Cell Adhesion Molecule (VCAM-1). These molecules interact in a highly specific manner to carry out certain functions. ICAM-3 expressed on leukocytes mediates endothelia-leukocyte contact through recognition of specific integrins on leukocytes. CD4 and CD8 molecules on T-cells bind to the Class I and Class II MHC molecules respectively, while the T-cell receptor (CD3) binds to the polymorphic antigen-presenting domain. This family also includes the Neural Cell Adhesion Molecule (NCAM). Homotypic interactions between two NCAMs on two adjacent cells mediate adhesion between them. Similarly, the Platelet and Endothelial Cell Adhesion Molecule-1 (PECAM-1) also uses homotypic interactions to establish contacts between adjacent endothelial cells and between leukocytes and endothelium as well as platelets.

CADHERINS

Cadherins are cytoskeletally linked membrane proteins that mediate cell-cell contact in many organs through homotypic binding to cadherins on adjacent cells, very much like NCAM and PECAM-1 molecules. Cadherin-mediated binding is calcium-dependent and is thought to play a very important role in development and in intercellular junctional structures (Perret et al. 2004; Salinas and Price 2005). They have not been described on blood cells but are found on endothelial cells where like PECAM-1, they help form cell junctions.

SELECTINS

The selectins are a family of cell adhesion molecules that play a crucial role in inflammation (McEver 2002; McEver 2004). Key chemical components released by macrophages and tissue mast cells fighting at the site of injury (or infection) induce the vascular endothelia to express selectins on their surfaces. The selectin family consists of three known members named according to their expression pattern: E-selectin is expressed on activated vascular endothelium; P-selectin is expressed on activated platelets but is also found on activated endothelia while L-selectin is expressed exclusively on leukocytes. Whereas L-selectin expression is constitutive, the expression of the vascular selectins (P- and E-selectin) is induced by inflammatory mediators and chemicals derived from tissue damage. P-selectin is stored in preformed granules in vessel endothelia (termed α-granules) as well as in platelets (termed Weibel-Palade bodies). Upon stimulation, the P-selectin is almost immediately transported to the vascular surface (McEver 1990). Unlike P-selectin, E-selectin is transcriptionally regulated with a peak expression after 4-6 hours of tissue damage or initial induction of inflammation.

Rapid transient binding and unbinding between the selectins and their ligands makes leukocytes slow down and roll along the vascular endothelia (Springer 1994) (Figure 1). During rolling, the leukocyte integrins are activated to a high-affinity state and firm adhesion of the leukocytes is established based on the binding between the leukocyte integrins and their ligands on the vascular surfaces. This brings the rolling leukocytes to a temporary halt and eventually, transmigration of the leukocytes across the endothelia into the tissue space is achieved by their amoeboid movement in the direction

of increasing chemoattractants concentration (McEver 1991; McEver 1994). Eventually, the leukocytes reach the site of infection by chemotaxis and participate in the process of phagocytosis. The highly regulated expression of the selectins helps initiate and terminate the inflammatory response. Dysfunction of selectin-ligand interactions leads to various inflammatory and thrombotic disorders (Springer 1985).

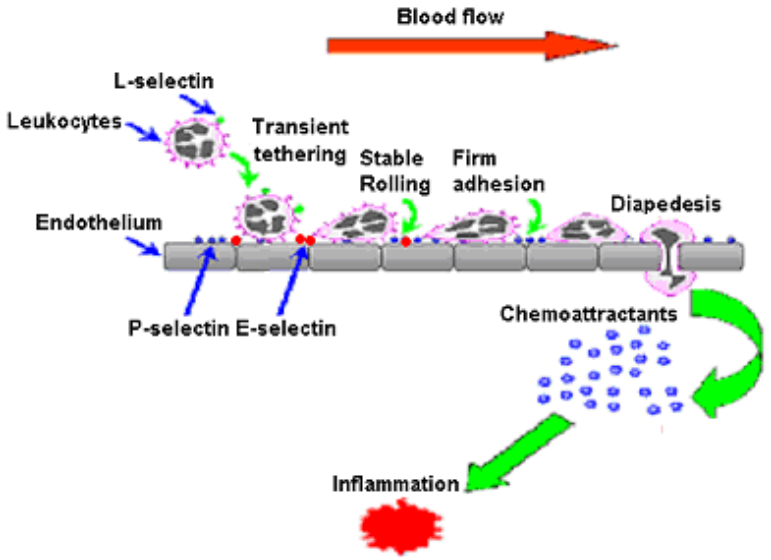

Figure 1: Inflammation Cascade

All the members of the selectin family have a common structure with a calcium-type Lectin domain at the N-terminus (Lectin), an epidermal growth factor-like domain (EGF-like), multiple copies of Consensus Repeats (CRs), whose sequences are homologous to the complement binding proteins (Johnston et al. 1989), a transmembrane domain (TM) and a short cytoplasmic tail (Cyt) (Figure 2). The major structural difference between the three selectins is in the number of CRs that they possess. P-selectin has 9 CRs; E-selectin has 6 while L-selectin is the shortest member, with only 2 CRs. High affinity binding between the selectins and their ligands requires specific

carbohydrate structures that are displayed on a limited number of membrane glycoproteins, the prototype of which is a tetrasaccharide called Sialyl Lewis-x (sLe^x) (McEver 1991). The best typified ligands for selectins are mucins that have a large number of clustered sialylated O-linked oligosaccharides. Site-specific construction of O-glycans with specific sialylated, fucosylated and in some cases, sulfated moieties is required for these mucins to serve as ligands for the selectins. The best biochemically characterized selectin ligand is P-selectin glycoprotein ligand 1 (PSGL-1) which has been shown to have very well defined physiological functions (McEver and Cummings 1997). It is a homodimeric sialomucin, about 60nm long and consists of two disulfide-linked, 120 kD subunits. Each subunit has at the most, 3 N-linked glycans but several clustered O-linked glycans. PSGL-1 serves as a ligand for all three selectins. In fact, selectin-PSGL-1 interaction serves as a prototype for other biologically relevant selectin-ligand interactions. L-selectin-PSGL-1 interactions have been implicated in the rolling of one leukocyte over another.

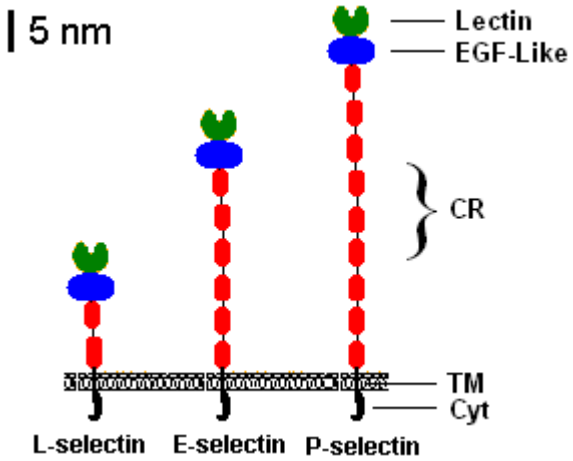

Figure 2: Selectins Structure

Apart from PSGL-1, other potential selectin ligands have been identified and even biochemically characterized in a few cases. For example, typical ligands for L-selectin include members of the CD34 family of sialomucins (CD34, Podocalyxin and Endoglycan) and Mucosal Addressin Cell Adhesion Molecule (MAdCAM) (Fieger et al. 2003). The CD34 family members have been proposed to be involved in processes as diverse as glomerular filtration, stem cell differentiation, leukocyte-endothelia adhesion and lymphocyte homing. The interaction between L-selectin and its ligands like CD34, MAdCAM etc occurs between endothelial cells and lymphocytes in the High Endothelial Venules (HEV). Typical ligands for E-selectin apart from PSGL-1 include E-selectin ligand-1 (ESL-1) and Sialyl Lewis-x (sLe^x).

2.2 Previous Studies Involving Selectins and Motivation for Current Work

Many independent research groups have embarked on studies involving the selectins. The tools employed by the different research groups vary and the prominent ones are flow chamber, micropipette and AFM. Different questions or issues concerning the selectins have been pursued and as a result, in the past decade or so, tremendous advancements have been made in the field of selectin biology. Several unexplored key issues concerning the selectins were identified and the specific aims for the current research work were duly formulated.

2.2.1 Mechanical Properties of Selectin-Ligand Complexes

The ability to predict binding affinities based on knowledge of the structure of a molecular complex is an important component in structural energetics problems like drug

design and development. Often, this requires information about the mechanical properties of the interactions in addition to the kinetics. Adhesive receptor-ligand complexes are often stretched by force because they link cells in mechanically-stressful environments, in which case, mechanical properties like complex elasticities may be highly relevant to their physiological function. However, very little is known about such properties. A previous study has reported the elasticity values of P-selectin-PSGL-1 complex, obtained using AFM (Fritz et al. 1998). But, the data and the interpretation of results have been obscured by very poor experimental design and control as well as the application of inappropriate models to fit the data. However, it should be duly noted that this group was the first to report such results.

Monomeric vs. Dimeric Interactions

Electron microscopy observations, biochemical assays and crosslinking studies have provided abundant evidence to suggest that leukocyte PSGL-1 is a dimer and cell surface P-selectin forms oligomers (Ushiyama et al. 1993; Barkalow et al. 2000; Epperson et al. 2000). Consistent with these data, flow chamber studies using mutant PSGL-1 that are no longer cross-linkable and soluble P-selectin that can no longer form oligomers have demonstrated clear differences in the lifetimes from the interactions of distinct forms of P-selectin and PSGL-1 (Ramachandran et al. 2001). By comparison, although L-selectin can be made dimeric by introducing a dimerizing motif to its cytoplasmic domain (Li et al. 1998), it is not known whether L-selectin naturally forms oligomers on the cell surface, and if so, whether oligomeric L-selectin supports dimeric bonds with native PSGL-1. Previous studies involving P-selectin have been performed

using AFM in our lab (Marshall et al. 2003). The data supported the view that P-selectin formed dimeric interactions with dimeric PSGL-1 but only monomeric interactions with monomeric sPSGL-1, consistent with the above-mentioned studies. Due to the lack of any such published information about E- and L-selectin, we decided to pursue this line of questioning for the other two selectins as well.

Contribution of Selectins to Complex Compliance and Related Issues

For the P-selectin experiments using AFM carried out by Marshall et al. (B. T. Marshall Doctoral Thesis 2002), data analysis revealed that in the stretch experiments, bulk of the compliance came from the selectins with the ligand or the mAb acting as relatively stiffer components. It was a very convenient and a very efficient technique to use other selectins as molecular probes to corroborate the above findings. Hence, a comprehensive study to delineate the mechanical properties of selectin-ligand complexes was undertaken.

2.2.2 Catch-Slip Transitional Bonds in Selectin-mediated Interactions

In a seminal theoretical paper in 1978, George Bell first proposed that the off-rate of receptor-ligand interactions was exponentially related to the force on the linkage (Bell 1978). His idea stemmed from the data of isotropic solids in classical mechanics (Zhurkov 1965). One could think of an applied force tilting the energy landscape and accelerate dissociation of the non-covalent receptor-ligand bond. Mathematically, the Bell Model (Bell 1978) can be represented as:

$$k_{off} = k_{off}^{o} * \exp(af/K_B T)$$

Here, k_{off}^{o} represents the unstressed off-rate (i.e. the off-rate in the absence of any applied force, *f*), K_B is the Boltzmann constant and T is the absolute temperature (in K). The parameter *a* is a parameter similar to the degree of dislocation in metals and polymers (Zhurkov 1965). Bonds whose *Off-rate vs. Force* characteristics was consistent with this theory are termed slip bonds. While this theory appeared very intuitive (namely the faster you pull, the faster the link snaps off), a rather controversial concept was put forth ten years later by Dembo et al. (Dembo et al. 1988). Dembo et al. proposed a theoretical finger-prison model, wherein force could allow more inter-locking of the receptor-ligand binding pocket. Such a force-induced conformational change could, then, result in a deceleration of bond dissociation. Those bonds, whose off-rates decrease with applied force, are termed catch bonds.

Slip bonds have been reported in a number of research studies (Alon et al. 1995; Alon et al. 1996; Alon et al. 1997; Lawrence 1999) and catch bonds existed only as a mathematical possibility. However, very recently, counter-intuitive catch-slip transitional bonds were documented in P-selectin-(s)PSGL-1 interactions, using AFM (Marshall et al. 2003). It was observed that at very low forces, not been previously considered, the lifetimes (which is the inverse of off-rates) of the P-selectin-(s)PSGL-1 bonds increased with increasing force (catch bonds). After a certain point, the lifetimes dropped precipitously with force, consistent with the slip bond behavior. This was not an experimental artifact of the AFM as independent flow chamber studies also confirmed this fact (Marshall et al. 2003). In order to understand whether these catch-slip transitional bonds were inherent to selectin-ligand molecular systems only, control experiments wherein P-selectin was interacted with an anti-P-selectin mAb, G1 were also

performed. Surprisingly, these interactions exhibited only slip bonds (Marshall et al. 2003). Thus, it was surmised that catch-slip transitional bonds were unique to selectin-mediated interactions. To further dissect this issue, L-selectin interactions with different ligands as well as an anti-L-selectin mAb were tested.

2.2.3 Force History Dependence of Receptor-Ligand Dissociation

For forced unbinding of receptor and ligand, the off-rate and force are related by the Bell model wherein off-rate is a single-valued function of applied force only (Bell 1978). Interestingly, the *Lifetime vs. Force* relationships obtained from flow chamber studies have been found to be differ drastically from those obtained from AFM experiments for the same receptor-ligand pair, e.g., P-selectin interacting with PSGL-1 (Alon et al. 1995; Fritz et al. 1998). This could be due to the fact that the results were obtained by different labs using different sources of reagents.

Previous studies in our lab involving P-selectin and PSGL-1 have revealed that for experiments performed by the same experimenter using the same sources of reagents and same experimental technique (AFM), the off-rates obtained from two different AFM assays differ not just quantitatively but also qualitatively (Marshall et al. 2005). This cast initial doubt on the predictions based on the Bell model and the putative relationship between off-rate and force. More detailed analyses revealed that the off-rate depended not just on force but actually on the entire force history or the path via which the force was reached (Marshall et al. 2005). It was argued that work done by an applied force would tilt the energy landscape (principle of superposition), accelerating dissociation. Though true for a point function like the instantaneous force, this would not necessarily

be true for path functions like work. Also, the concept of superposition can only be applied to conservative work and not for dissipative work like friction. In such a case, dissociation kinetics would depend on the entire history of force application, which would then give rise to a path-dependence of off-rate (Marshall et al. 2005). The concept of force-history dependence appeared more deep-seated than force dependence of off-rate; for the latter is a special case of the former if the force histories are restricted to those with constant forces only. This generalized concept reconciled the apparent discrepancies in the *Off-rate vs. Force* relationships obtained from the different AFM assays.

It was tough to assimilate and digest the concept of force history due to several reasons. First of all, it challenged a ~ 25-year old paradigm, namely the Bell model (Bell 1978). Secondly, being relatively new-fangled, this concept had not been tested or proved for other receptor-ligand systems. Thirdly, the work by Marshall et al. compared results obtained from two different AFM assays and it was increasingly difficult to get the point across without too much of an ambiguity. In order to set this issue right, we decided to design simple and relatively straight-forward experimental assays. With this idea in mind, L-selectin interactions with monomeric sPSGL-1 and 6-sulfo-sLe^x were tested and the results carefully analyzed for the existence of any force history.

2.3 Atomic Force Microscopy (AFM)

Atomic force Microscopy (AFM) was developed in the mid 1980s and has since then, evolved to be a powerful tool to probe the interaction forces between sample specimens on the cantilever tip and apposing surfaces (Binnig 1986). The ability of the

AFM to achieve high resolution (nm distance and pN force) has made it a very handy tool for biological applications as well. Every conceivable biomaterial has been explored using the AFM. In addition, the AFM has also been extensively used in various biological applications like DNA, RNA and protein imaging. As far as the non-imaging applications of the AFM are concerned, force studies between antigen-antibody complexes and receptor-ligand complexes as well as protein dynamics have also been actively pursued (Florin 1994; Dammer 1996). Biotin-avidin was the first receptor-ligand pair to be studied using AFM. Since then, many groups have used the AFM to characterize other receptor-ligand interactions as well. During inflammation, selectin-ligand bonds form and break under mechanically stressful hydrodynamic conditions *in vivo*. It was thus, imperative to characterize these interactions under very similar conditions *in vitro*, which was possible due to AFM. The approach and retraction of the AFM cantilever decorated with a ligand over a selectin-incorporated lipid bilayer can be likened to a leukocyte approaching and departing from the endothelia.

2.4 Overall Significance of the Project

A central goal of cellular bioengineering is to understand cell behavior in terms of molecular properties. In this regard, characterizing the interactions between receptors and ligands assumes significance. In the field of pharmacokinetics, effective drug design and development is made possible through a systematic understanding of the underlying molecular properties. Dynamic models of selectin-ligand interactions could be used for the development of selectin-based anti-inflammatory drugs. Data obtained from this

project will not only add to the existing body of knowledge but also provide new insights into mechanisms by which selectins initiate leukocyte adhesion under shear.

CHAPTER 3

MATERIALS AND METHODS

3.1 Proteins and Antibodies

P-, E- and L-selectins were respectively purified from human platelets, transfected Chinese hamster ovary (CHO) cells and human tonsils (Moore et al. 1992; Lawrence et al. 1997). Native dimeric PSGL-1 was purified from human neutrophils (Moore et al. 1992). Recombinant monomeric soluble PSGL-1 (sPSGL-1) was purified from CHO cell transfectants (Yago et al. 2002). The Endoglycan-Ig, which consists of the extracellular region of the molecule fused to a human Fc domain, was collected from transfected COS7 cell supernatants (Fieger et al. 2003). The blocking anti-P-selectin mAb G1 (Geng, et al. 1990), anti-L-selectin mAb DREG56 (Kishimoto et al. 1990) and the blocking (PL1) and capture (PL2) anti-PSGL-1 mAbs have been described (Moore et al. 1995). Anti-P-selectin mAbs S12, W40, 5A8 and 2B8 and anti-E-selectin mAb ES1 were purified from supernatants of the respective hybridomas. Biotinylated 2-GSP-6 and its functional analog 2-GP-1 were generous gifts from Dr. Richard Cummings (Oklahoma University Health Sciences Center, Oklahoma City, OK).

3.2 The AFM System

The AFM system was built and calibrated in house (design adapted from Vincent Moy, University of Miami) (Figure 3A) (Marshall, Long et al. 2003). It consists of a piezoelectric translator (PZT) (Polytec Physik Instrument, Boston, MA) on which a cantilever [Thermomicroscopes (presently Veeco, Santa Barbara), Sunnyvale, CA] is

directly mounted. A laser (Oz optics, Ontario, Canada) focused on the end of the cantilever's back is deflected onto a photodiode (Hamamatsu, Bridgewater, NJ) that measures the quasi-static tip inclination that is directly proportional to the quasi-static tip deflection, which is converted to force using the cantilever spring constant. Each cantilever spring constant (4-100 pN/nm) was calibrated during the experiment using thermal fluctuation analysis (Hutter and Bechhoefer 1993). A personal computer with a data acquisition board (National Instruments, Austin, TX) was used to control the movement of the PZT and to collect the signal from the photodiode. LabView (National Instruments) was used as the interface between the user and the data acquisition board.

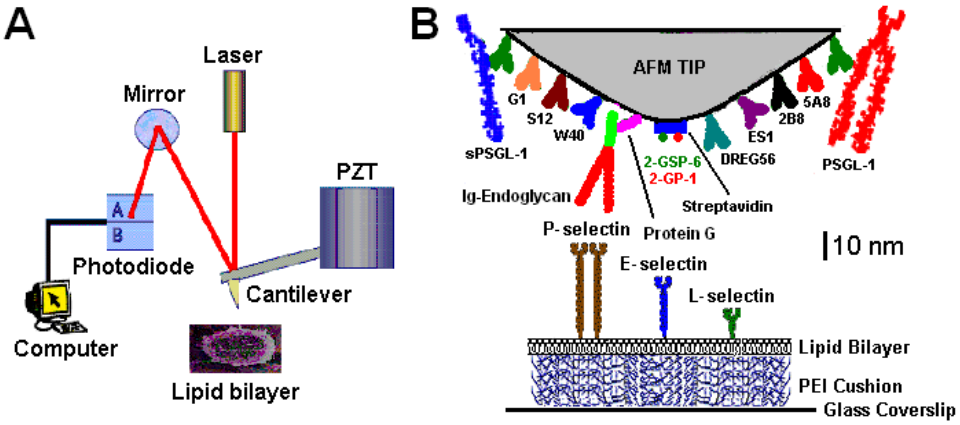

Figure 3: (A) AFM Schematic (B) Experimental Set-up

3.3 Functionalization of AFM Cantilever Tips

Different cantilever tips were incubated overnight at 4 °C in 10 µl of 10 µg/ml of PL2, Protein G, streptavidin, selectin-specific mAbs or 1 % bovine serum albumin (BSA), during different experiments. After rinsing, the coated cantilevers were incubated for 30 min at room temperature in Hanks' balanced salt solution (HBSS) or Dulbeccos' Phosphate Buffered Saline (DPBS) containing Ca^{2+} and Mg^{2+} ions and 1 % BSA to block

nonspecific adhesion. PL2- (or Protein G- or streptavidin-) coated cantilevers were further functionalized by incubation in 10 µl of 100 ng/ml (s)PSGL-1 (or Endoglycan supernatant or biotinylated 2-GSP-6 or 2-GP-1) for 20 min at room temperature. Antibody-, BSA-, and some PL2- and Protein G-coated cantilevers were used without further modification (Figure 3B).

3.4 Preparation of Selectin-incorporated Liposome Solutions

A selectin-incorporated lipid vesicle solution was prepared following the method of McConnell et al. (McConnell, Watts et al. 1986; Dustin, Olive et al. 1989). Briefly, vesicles were formed by hydrating a dried lipid film of egg phosphatidylcholine (PC) (Avanti Polar Lipids, Alabaster, AL) with 2 % Octyl β-Glucopyranoside (OG) (Fisher Scientific, Pittsburgh, PA) Tris saline solution creating 250 µl of 0.8 mM lipid solution. The 2 % OG egg PC solution was combined with 250 µl of 1 % OG solution with a 28 µg/ml concentration of membrane selectin. The resulting 0.4 mM lipid solution was dialyzed with three 1-liter changes of Tris saline buffer (25 mM Tris-HCL, 150 mM NaCl, pH 7.4) in 12 h increments. The resulting lipid vesicle solution was stored under argon at 4 °C and used within several months.

3.5 Formation of Selectin Bilayers

In the AFM experiments, forces as low as thermally-driven force fluctuations were frequently encountered, which are smaller than the adhesion forces between coverslips and SiN_3 cantilever tips, yielding ~100 % nonspecific binding because all nonspecific interactions can be detected (Marshall et al. 2003). Covering the glass with

an intact lipid bilayer reduced the nonspecific binding to nearly zero. Nonspecific binding was increased when any of the selectins was incorporated in the bilayer, presumably because it was partly disrupted by the inversely inserted selectins that have extracellular domains much larger than the normal gap distance between the bilayer and the coverglass. It was, hence, crucial to add a PEI cushion to accommodate the inversely oriented molecules between the glass and the bilayer (Figure 3B), which reduced the non-specific binding to ~ 5 % (cf. Figure 16).

40 mm diameter coverslips (Bioptechs, Butler, PA) were cleaned using a mixture of a 70 % 12N sulfuric acid and 30 % hydrogen peroxide by volume mixture at a temperature of 100 °C for 45 min, rinsed extensively with deionized water, and dried completely under an argon stream. The cleaned coverslips were stored in a desiccator and used within a two-week period. During each experiment, a clean coverslip was first immersed in a 100 ppm PEI (MW = 1800 g/mol, 95 % purity; Polysciences, Warrington, PA) solution of 0.5 mM KNO_3 (Fisher Scientific, Pittsburgh, PA) in deionized water (pH 7.0) for 20 min. After rinsing, excess water was removed from the coverslip surface by a gentle stream of argon. The coverslip was then placed in a desiccator for 10 min to dry the PEI layer before forming a selectin bilayer on it (Wong et al. 1999; Wong et al. 1999; Marshall et al. 2003).

Bilayers were formed using the method of vesicle fusion (McConnell et al. 1986; Dustin et al. 1989). A 4 µl drop of selectin-incorporated lipid vesicle solution was placed on the surface of the PEI-coated coverslip. After 20 min incubation under a damp paper towel, the Petri dish was filled with 10 ml HBSS or DPBS containing Ca^{2+} and Mg^{2+} ions and 1 % BSA. The selectin bilayers so formed had low molecular densities, which

ensured their infrequent binding to the (s)PSGL-1-, Endoglycan-, 2-GSP-6 or mAb-coated cantilever tips, as required for measuring single bond interactions. Bilayers were immediately used in AFM experiments. During each experiment, the bilayers were first tested for quality using yet-to-be functionalized or Protein G- (or streptavidin- or BSA-) coated tips for low nonspecific binding.

3.6 Calibration of Cantilever Spring Constant

During each experiment, the cantilever spring constant (4-100 pN/nm) was calibrated using the method of thermal fluctuation analysis (Hutter and Bechhoefer 1993). Two corrections were made to further improve the accuracy of the cantilever spring constant estimations. The first had to do with the fact that the photodiode monitored laser light bounced from the back of the cantilever tip, which measured the cantilever tip inclination rather than the cantilever tip deflection. The second correction had to do with the finite bandwidth of the photodiode signals, which limited the number of observable resonant frequencies in the measured spectral density plot to no more than three, thereby, over estimating the spring constant value. The need for the above two forms of corrections were evident from the fact that in some cases, the cantilever spring constants were over estimated by as much as ~ 50 %.

3.7 AFM Adhesion Event and Force & Lifetime Measurements

Binding was enabled by driving the cantilever tips with the PZT to contact the bilayers for 2 s with a ~ 30 pN compressive force. The cantilevers were then retracted at constant set speeds that varied between 250 and 25000 nm/s in different experiments. The

absence or presence of adhesion was detected from the force-time scan curves (Figure 4A and B). When the tip was linked to the bilayer by a molecular bond, continued cantilever retraction yielded tensile forces that signified binding, which were clearly visible from the force-time scan curves (Figure 4B). Adhesion frequency was defined as the number of binding events per 100 repeated approach-retraction cycles using the same tip contacting the same bilayer spot.

Data were collected along two families of loading paths: constant-rate loading, where force increased linearly with time until the bond ruptured (Unbinding Force Assay) and constant-force loading, where force initially increased linearly with time and then became constant once a prescribed level was reached (Lifetime Assay). Unbinding forces were measured along the former loading paths (Figure 4B) while unbinding forces and bond lifetimes were measured along the latter (Figure 4C and D). Lifetime measurement started from the instant the PZT stopped to the instant of bond failure (Figure 4C and D).

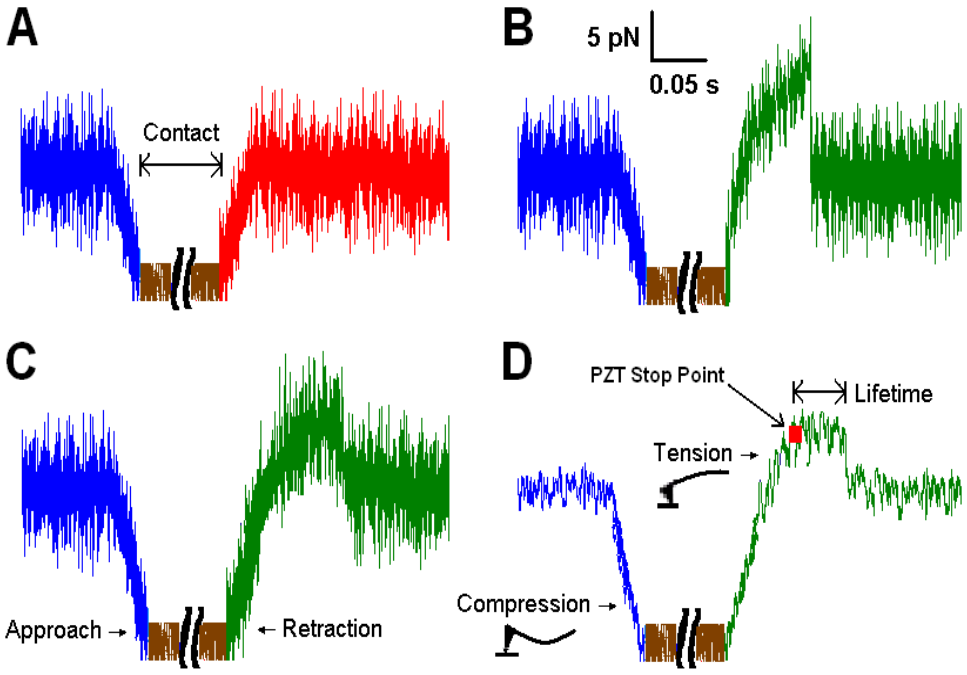

Figure 4: Characteristic Force-Time Scan Curves

Unbinding force data were acquired at 1.5 kHz and lifetime data were acquired at 3-5 kHz. Most of the lifetimes were tens of milliseconds or longer and hence, a number of instantaneous forces were averaged to allow lifetime measurement at forces comparable to the level of thermal fluctuations (Marshall et al. 2003). Figure 4D exemplifies how the amplitude of force fluctuations in Panel C was reduced by a sliding average of 10 points, such that the levels of force-time scan traces before and after the rupture event no longer overlapped. This was equivalent to trading the temporal resolution (reduced from 0.2 to 2 ms) for the force resolution.

3.8 Calculation of Complex Elasticities

Complex elasticities were measured using the stretch method. In this method, the complex elasticities were directly measured from the *Force vs. Molecular Extension* curves when the selectin-ligand (or -mAb) complexes were stretched, assuming they behaved as linear springs (Figure 5). Since the PZT retracted the built-in end of the cantilever at a constant speed low enough to neglect the cantilever inertia and viscous drag, the mean photodiode signal measured the quasi-static tip inclination that was directly proportional to the quasi-static tip deflection. Force was directly measured by $f = k_c\langle z\rangle$ (k_c - cantilever spring constant; $\langle z\rangle$ - cantilever deflection) and the molecular extension z_m was calculated by subtracting $\langle z\rangle$ from the PZT movement z_{pzt}, i.e., $z_m = z_{pzt} - \langle z\rangle$. Complex elasticity, thus, would be f / z_m. In essence, in this method, the coupled system behaved as if the cantilever spring and the molecular spring were in series. For all the molecular systems examined, the ascending phase(s) of the *Force vs. Molecular Extension* plots were nearly linear (red trend lines) and the molecular elasticities were

determined from the slopes of the curves in the ascending portions (Figure 5). Few tens of measurements were made for each molecular system and the data were presented as Mean ± S.E.M.

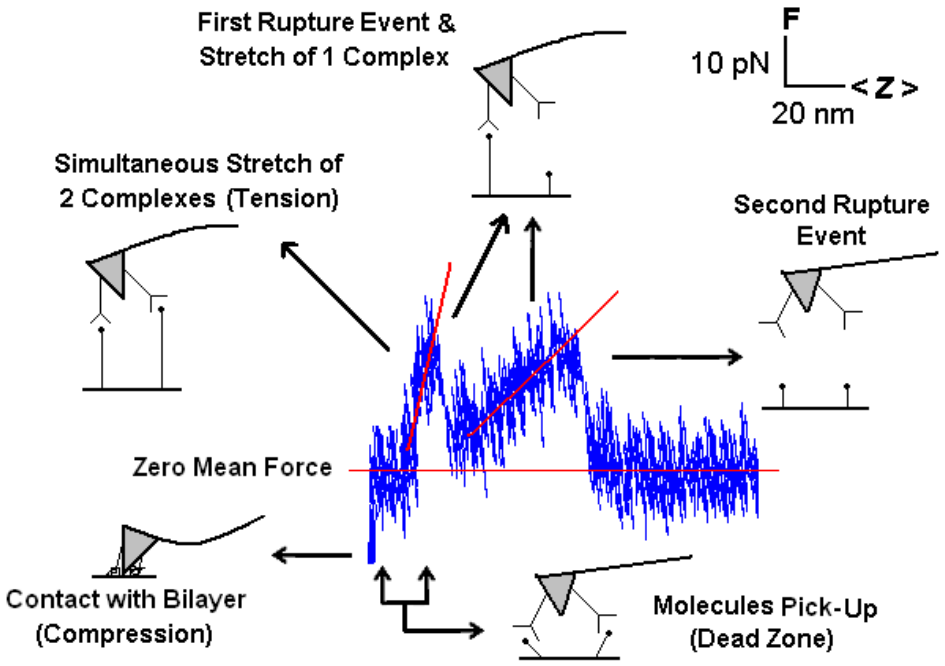

Figure 5: Calculation of Complex Elasticities and Dead Zone

3.9 Dead Zone Measurements

In some of the adhesion events, a regime with a zero-mean force between the compressive and tensile force regimes was observed (Figure 5). In this regime, the PZT continued to retract without any visible cantilever bending and the cantilever tip and base moved concurrently. Since only some of the adhesion events displayed a dead zone, it was hypothesized that the dead zone could not be due to an inherent mechanical property of the molecular complexes being stretched. In order to fully understand what the dead zone truly represented, the dead zone distributions of several molecular systems were

analyzed. A systematic analysis revealed that the dead zone represented a regime wherein the molecules were being picked up and re-oriented along their long axes before stretch, after being squashed during the compressive contact phase (Figure 5).

3.10 Analysis of Bond Lifetimes

Lifetimes were analyzed using the first-order dissociation kinetics model, $B \xrightarrow{k_{off}} R + L$, where R, L, and B denote, respectively, receptor, ligand, and bond. For lifetimes measured at constant force (f), the off-rate, k_{off} was assumed to be a constant at each force and independent of time (t). This model predicts that lifetimes of single bonds are exponentially distributed, $p = \exp[-k_{off}(f)t]$, where p is the probability of a bond observed at time 0 that would remain intact at time t. Taking the semi-log would linearize the exponential distribution and the slope of the *Ln(# of events with a lifetime > t) vs. t* plot would equal $-k_{off}$, the negative reciprocal of which would yield the bond lifetime.

It was observed that the individual lifetime data were scattered. This scattering of the data was not a reflection of the lack of measurement accuracy, which was better than 1 ms for the AFM experiments. Rather, it was a manifestation of individual molecular bond dissociation, which is stochastic by nature. Thus, the standard deviation $\sigma(t)$ were not used as error bars because it measured a statistical property of the probability distribution rather than the uncertainty in the data. Indeed, it can be easily shown that $\sigma(t)$ of an exponential distribution is equal to the mean $\langle t \rangle$, both of which equal $1/k_{off}$.

Several methods were employed to assess the statistical significance of the differences in the k_{off} values estimated at different forces, especially in the force range

where catch bonds were observed. First, individual AFM experiments were performed to measure a few lifetimes at each of several force levels that covered the entire force range. The lifetime at each force level was estimated from the mean and the standard deviation of these measurements. It was found that the *Lifetime vs. Force* curves so obtained were stable as soon as the number of measurements reached ~ 100. To ensure statistical stability, 350-450 measurements were made for each system. The statistical significance of differences between any two neighboring points in the range where the majority of the data resided were determined by the F-test that compared the slopes of the two *Ln(# of events with a lifetime* $\geq$ *t) vs. t* data.

CHAPTER 4

SPECIFIC AIM #1: DELINEATING THE MECHANICAL PROPERTIES OF SELECTIN-LIGAND COMPLEXES

During inflammation, selectins mediate the transient sticking of leukocytes to hyper-adhesive vascular surfaces. Stretched by the flowing blood, selectin-ligand bonds link cells in a mechanically stressful milieu and their mechanical properties are likely pertinent to their physiological function. In order to delineate the mechanical features of these molecular complexes, the elasticities and *Force vs. Molecular Extension* behaviors of three selectins complexed with different ligands and selectin-specific monoclonal antibodies (mAbs) were measured using AFM. Different ligands and mAbs were used to interact with different selectins at different domains (*cf.* Figure 3B and Figure 6). Experiments were performed by repeatedly moving the ligand or the antibody-coated tips into and out of contact with the selectin bilayers.

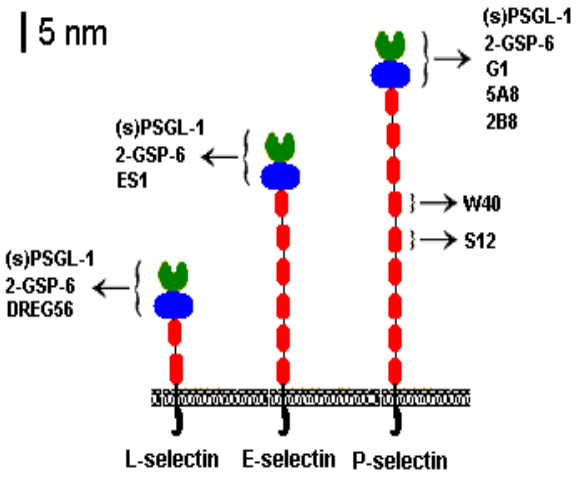

Figure 6: Binding epitopes of Ligands or Antibodies

During each experiment, the selectin-incorporated bilayer was first, tested for quality using non-functionalized or BSA-coated tips. Whenever the non-specific binding frequency was ≤ 5 %, the AFM cantilever tips were further functionalized with ligands or the BSA-coated tips replaced by mAb-coated tips and the experiments were continued to confirm the substantial increase in adhesion frequencies.

For the specific adhesion events, the number of null, single, double and triple rupture events followed Poisson distribution in accordance to small number statistics (*cf.* Figure 24). To ensure that the measured values represented properties of individual molecules instead of their clusters, binding frequency was kept to a minimum (~ 15-20 %). Complex elasticities were determined from the *Force vs. Molecular Extension* curves by stretching the molecular complexes, assuming they behaved as linear springs (Figure 5). On a few occasions, double and triple break events were observed, which represented respectively, two and three single bonds being loaded in parallel, from which the elasticities of double and triple bonds were determined. Tens of measurements were made for each molecular system and data were expressed as Mean ± S.E.M.

In some adhesion events, a dead zone corresponding to a zero-force regime between the compressive and tensile force regimes was observed (Figure 5). Since, not all the adhesion events displayed a dead zone, it was hypothesized that the dead zone was not an inherent mechanical property of the molecular complexes. The dead zone characteristics of various selectin-ligand (or mAb) systems were looked at to understand what the dead zones truly represented.

4.1 Results

4.1.1 Efficacy of AFM in Probing Single Molecular Interactions

Bond ruptures were clearly visible from the force-time scan curves as discrete events (Figure 5). Under the infrequent binding conditions (~ 15-20 %), the frequency of rupture events appeared as null, single, double, triple etc and followed Poisson distribution, as expected from small number statistics (data not shown). While it was necessary to keep binding infrequent, Poisson statistics alone was insufficient to guarantee that the apparently discrete interactions were single bonds. To begin with, the dead zone distributions were carefully analyzed. Since, not all the adhesion events displayed a dead zone, it was hypothesized that the dead zone occurred because a molecule had to be picked up by its counter molecule, both of which had finite lengths. Further, the molecular complex had to be oriented and aligned along its long axis before it could resist tensile force that stretched it beyond its resting length, as schematically illustrated in Figure 5. For all molecular systems, histogram analysis revealed a bell-shaped distribution with the peak dead zone length closely matching the mean (Figure 7).

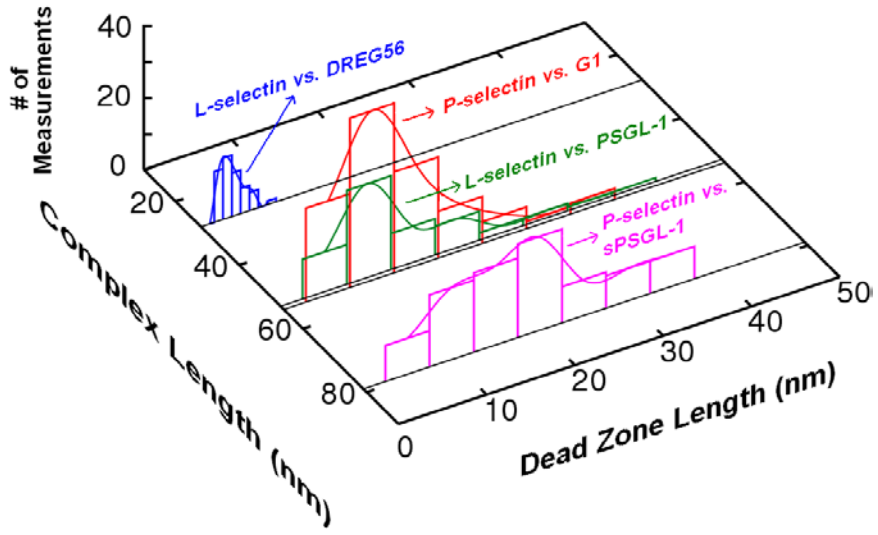

Figure 7: Histogram Analysis of Dead Zone Distributions

The mean dead zone lengths were found to be linearly correlated with the lengths of the molecular complexes stretched, regardless of the nature of the molecular interactions. This was observed in single as well as double break events (Figure 8). However, for the same molecular pair, the dead zone length for the double break events was smaller than that for the single break events (Figure 8: color-matched *open vs. closed* symbols). This was consistent with our initial hypothesis, as picking up, orienting, and aligning two molecules would pose additional geometrical constraints on the cantilever bending (Figure 5), which would reduce the dead zone length even for the same molecular complex length (Figure 8). Also, the dead zone always occurred prior to force build-up. So, if the individual breaks seen in Figure 5 were to represent unfolding of globular domains as opposed to bond rupture, the dead zone lengths for the single and double break events would have been identical, which was not the case.

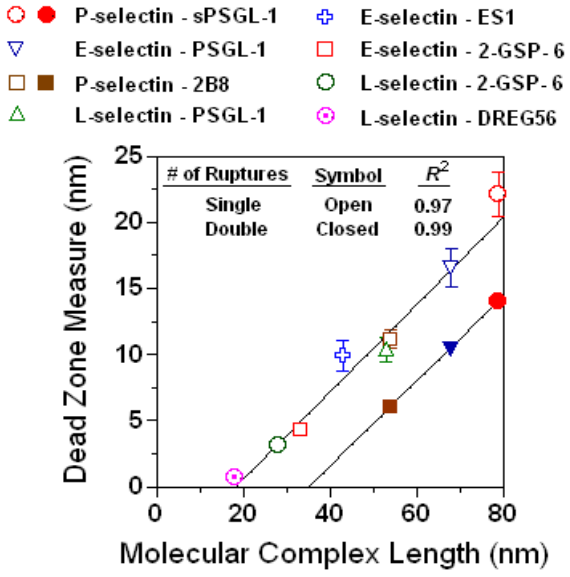

Figure 8: Dead Zone Measure vs. Molecular Complex Length

Secondly, in the *Force vs. Molecular Extension* curves, the slopes of the linear force build-up segments prior to the n^{th} rupture event increased linearly with n (Figure 9). Since these slopes are approximately equal to the complex elasticity, these rupture events represented unbinding of parallel bonds rather than unfolding of serial domains as in protein unfolding experiments (Kellermayer et al. 1997; Rief et al. 1997). This was further supported by quantitative measurements showing that the elasticities of the complex prior to the second and third rupture events were respectively, two and three times of that prior to the first rupture (in multiple rupture events) or the solitary rupture (in single rupture events). This quantal behavior suggested that each rupture event represented the unbinding of a single binding unit - a single bond or a cluster of a given number of bonds, whose individual member's dissociation could not be distinguished by the AFM experiments.

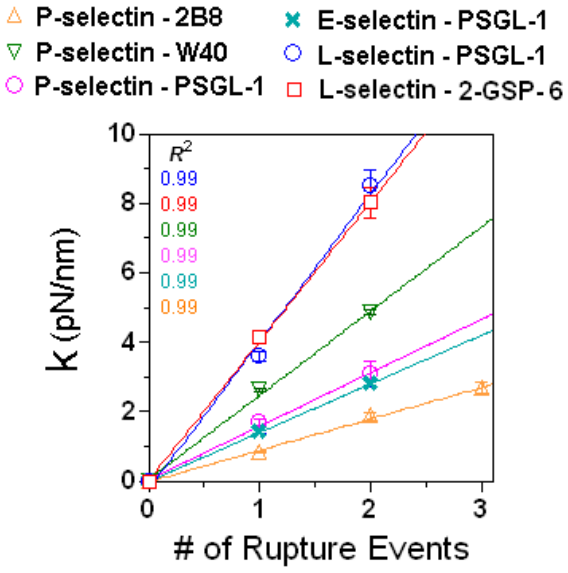

Figure 9: Quantal Behavior of Complex Elasticities

4.1.2 Monomeric vs. Dimeric Interactions

Electron Microscopy, biochemistry and crosslinking studies have provided abundant and convincing evidence that PSGL-1 and P-selectin are dimers on their respective cell surfaces, which enhances their adhesion under flow (Barkalow et al. 2000; Epperson et al. 2000; Ramachandran et al. 2001). Consistent with these observations, previous AFM studies have revealed that membrane P-selectin supports dimeric interactions with dimeric PSGL-1 but not with monomeric sPSGL-1, wherein a rightward and upward shift of the *Lifetime vs. Force* curve for the P-selectin-PSGL-1 system was observed relative to the P-selectin-sPSGL-1 system, doubling both the force *and* lifetime (Marshall et al. 2003). The idea of geometric constraints allowed us to use dead zone measurement to differentiate between monomeric and dimeric bonds. Consistent with the above-mentioned studies, for events with the same number of breaks, the dead zone lengths for P-selectin-PSGL-1 interactions were shorter than those for P-selectin-sPSGL-1, though the complex lengths stretched in the two cases were the same (Figure 10A). By comparison, the dead zone lengths for E- and L-selectins were indifferent to the form of PSGL-1 used, suggesting that the same monomeric bonds were formed for E- and L-selectin interacting with either form of PSGL-1 (Figure 10A).

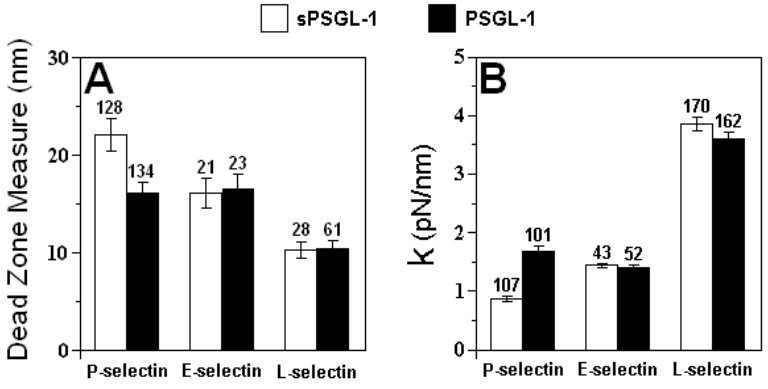

Figure 10: Monomeric vs. Dimeric Interactions

Previously, molecular elasticity measurements suggested that P-selectin formed dimeric bond with PSGL-1 but monomeric bond with sPSGL-1, as the elasticity of the P-selectin-PSGL-1 complex was double that of the P-selectin-sPSGL-1 complex (Figure 10B). This was not due to the formation of double bonds since the binding frequencies were maintained at the same level (~ 15-20 %) in all experiments. Moreover, double bonds were seen as double breaks representing two unbinding events (*cf.* Figure 5), while a dimeric bond was seen as a single rupture event (P-selectin studies were done by Dr. Bryan Marshall). It was found that like the dead zone measurements, the elasticities were identical for E- and L-selectin interacting with both forms of PSGL-1 (Figure 10B). This regular consistency between the dead zone and elasticity measurements provided strong evidence that membrane E- and L-selectins, unlike P-selectin, did not support dimeric interactions with dimeric PSGL-1 under the conditions tested.

Additional experiments were performed using a 19 amino acid-long synthetic PSGL-1-mimic called 2-GSP-6 and its control analog, 2-GP-1 (both with a single biotin at their C-terminal ends). In these experiments, the three selectins were tested against different cantilever tips functionalized with varying proportions of functional 2-GSP-6 and non-functional 2-GP-1 captured using streptavidin, which was adsorbed on the AFM tip (*cf.* Figure 3B). Streptavidin presents four binding sites, two on each side of which it is possible that two of those sites are blocked when the streptavidin gets adsorbed on the AFM tip. Binding to the two exposed sites on streptavidin would assemble two monomeric 2-GSP-6 molecules into a dimer (Figure 11). Hence, incubating the AFM cantilevers with varying proportions of 2-GSP-6 and 2-GP-1 would give rise to varying probabilities of sustaining monomeric and dimeric bonds.

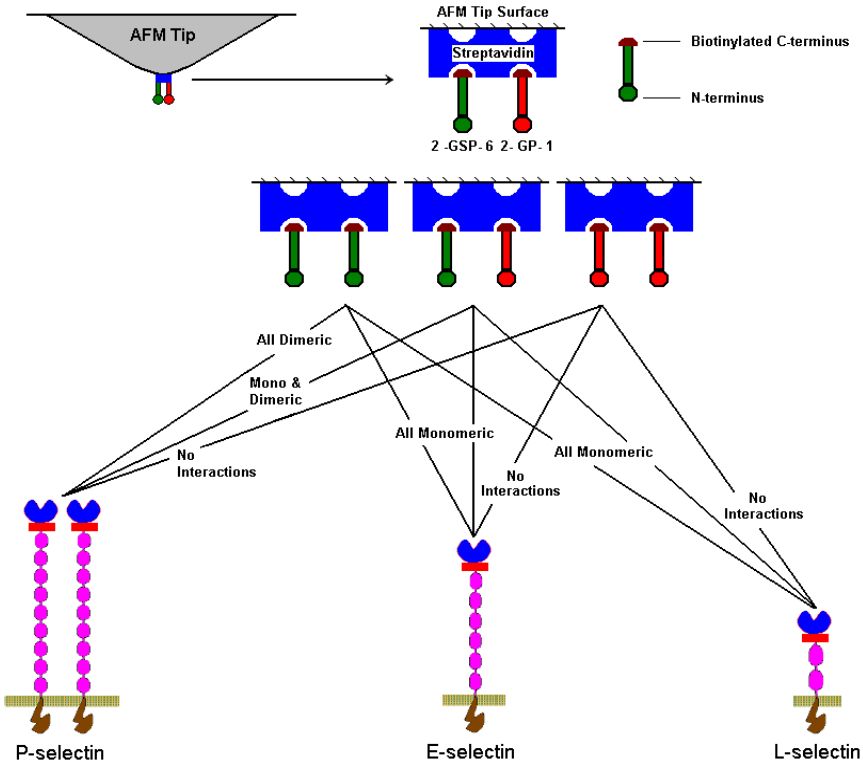

Figure 11: Cartoon Depiction of 2-GSP-6/2-GP-1 Capture on AFM Tip

For the P-selectin-2-GSP-6 systems, for events with the same number of breaks, the mean dead zone length monotonically decreased with increasing 2-GSP-6 %, indicating a progressive increase in the proportion of dimeric bonds. However, the decrease was not striking, with the values not being statistically very different (data not shown). This was in spite of the fact that the complex lengths being stretched were the same in all the cases (Figure 12A). By comparison, the dead zone lengths for E- and L-selectins were indifferent to the % of 2-GSP-6 used (Figure 12A), suggesting that the valency of the bonds formed in the different cases for each selectin were the same (in these cases, monovalent). Also, only for P-selectin-2-GSP-6 systems, the mean complex elasticities increased monotonically with increasing 2-GSP-6 %, again suggesting a progressive increase in the % of dimeric bonds (Figure 12B), suggesting that the

difference in their behaviors were due to the dimerization of P-selectin and its ability to sustain dimeric interactions with the artificially created dimeric 2-GSP-6.

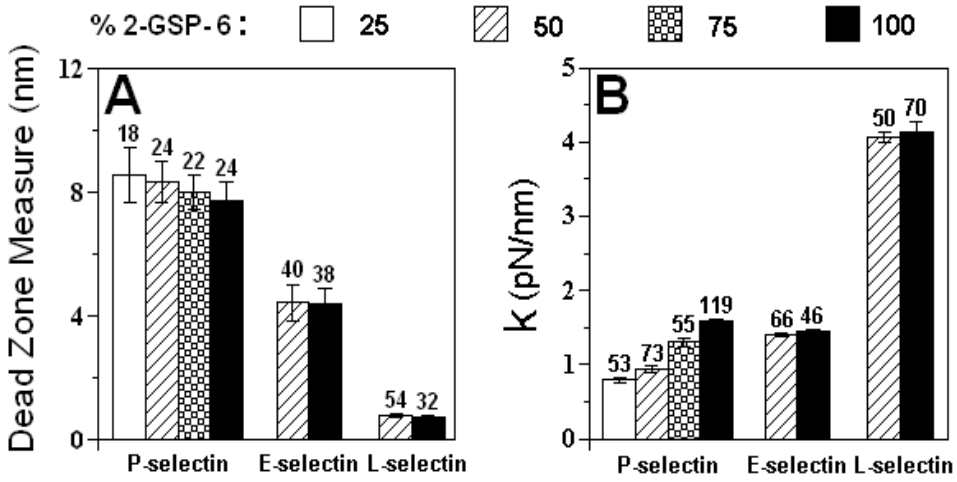

Figure 12: Effect of % 2-GSP-6 on Dead Zone and Elasticities

For P-selectin interacting with 100 % 2-GSP-6, the elasticity histogram displayed a single peak whose location coincided with the elasticity measure of P-selectin-PSGL-1 system (*cf.* Figure 10B and Figure 13D). By comparison, the histograms for the various P-selectin-2-GSP-6/2-GP-1 ratio systems all exhibited two peaks located at one and two times a common value, again, revealing a quantal behavior (Figure 13 A-C). Interestingly, the positions of these peaks coincided with the elasticity values of the P-selectin-sPSGL-1 and P-selectin-PSGL-1 systems respectively (*cf.* Figure 10B and Figure 13 A-C). This quantal behavior seen in histograms of the hybrid 2-GSP-6/2-GP-1 systems, thus, suggested that the positions of the peaks corresponded to the elasticities of the monomeric and dimeric P-selectin-(s)PSGL-1 complexes respectively. On the other hand, for E- and L-selectin, all the distributions were marked by the presence of a single peak (Figure 13 E-H), which denoted the elasticities of these monomeric complexes and

as before, these values coincided with the elasticity measures of the respective selectins complexed with either form of PSGL-1 (*cf.* Figure 10B).

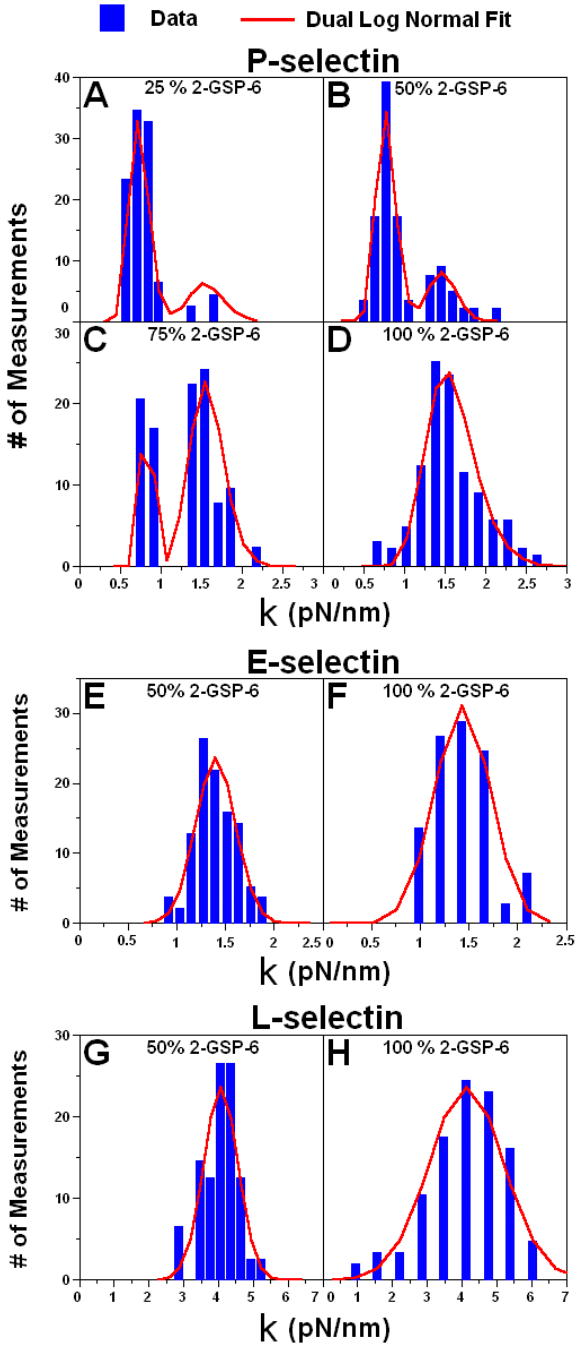

Figure 13: Elasticity Histograms of Selectin-2-GSP-6/2-GP-1 Systems

For P-selectin, the relative areas under the two peaks varied with the relative proportions of monomeric and dimeric 2-GSP-6, suggesting the varying relative amounts of monomeric and dimeric interactions. Furthermore, the area under the second peak (relative to the first peak) increased with increasing 2-GSP-6 content (Figure 13 A-C). The numbers of 2-GSP-6 and 2-GP-1 molecules captured on the AFM cantilever tips were calculated based on the ratios of the mixtures used, which would be related to the relative fractions of monomeric and dimeric 2-GSP-6. It was assumed that these numbers (and hence, the relative fractions) would directly correspond to the probability of sustaining monomeric and dimeric bonds. The histograms were then, fitted by a dual log normal distribution model with the mean of one of them twice that of the other. It was found that this model fit the experimental data very well (Figure 13 - solid red curves in all panels). Collectively, all the above information suggested that for P-selectin, a quantal binding unit consisted of a monomeric and dimeric bond while interacting with sPSGL-1 and PSGL-1, respectively. In the cases of E- and L-selectin, the measured interactions with (s)PSGL-1 and 2-GSP-6/2GP-1 ligand systems always represented monomeric bonds, which comprised the smallest binding unit.

4.1.3 Contribution of Ligands (or mAbs) to Complex Elasticity

To delineate the relative contributions of the different components to the measured elasticities, the changes in elasticities when some of the elements were replaced or removed were examined. Anti-PSGL-1 mAb PL2, anti-P-selectin mAbs G1, 5A8, 2B8, S12 and W40, anti-E-selectin mAb ES1 and anti-L-selectin mAb DREG56 are all mechanically similar in that they are all mouse IgGs (IgG1 sub-kind). Barring PL2, all other mAbs bind

at or near the Lec-EGF domain of the respective selectin and hence, block interactions of the selectin with PSGL-1. As such, the contribution of the selectin molecule would be the same irrespective of whether it was bound to PSGL-1 or an antibody. Thus, the selectin-mAb system is mechanically equivalent to removing the PSGL-1 molecule from the selectin-PSGL-1-PL2 serial system and one would expect the complex elasticity to increase. Contrary to this, it was observed that removing the PSGL-1 molecule in no way affected the elasticities for all selectin cases (Figure 14A). Along similar lines, selectin-2-GSP-6 system is mechanically equivalent to replacing the full-length ~ 280-amino acid long PSGL-1 molecule with a short 2-GSP-6 with only 19-amino acids (~ 15-fold reduction in length) plus replacing the PL2 with a much shorter streptavidin molecule. Again, introduction of these changes did not impact the elasticity measures (Figure 14A). This suggested that in the stretch experiments, the selectins were the major contributors to the complex compliance.

4.1.4 Effect of Selectin Molecular Length on Elasticity

While remaining unaffected by the changes in the ligands, the elasticities of the three selectin systems interacting with the same ligand, sPSGL-1, were different: lowest for P-selectin (~ 0.8 pN/nm), intermediate for E-selectin (~ 1.4 pN/nm) and highest for L-selectin (~ 4.2 pN/nm) (Figure 14B). A major structural difference between the three selectins is the number of consensus repeats (CRs) that determine the length of each selectin (*cf.* Figure 6). The observation that the elasticities were inversely related to the length of the selectin, thus suggested the CRs to be the major contributors to the selectin compliance. To further characterize the contribution of the CRs, elastic constants of P-

selectin complexed with two mAbs (W40 and S12) that bind respectively the 4th and the 5th CRs (from the N-terminus, *cf.* Figure 6) were measured. As expected, higher elasticity measurements (2.6 pN/nm and 2.5 pN/nm respectively) were obtained as in these experiments, only part of the P-selectin molecule was stretched (Figure 14C).

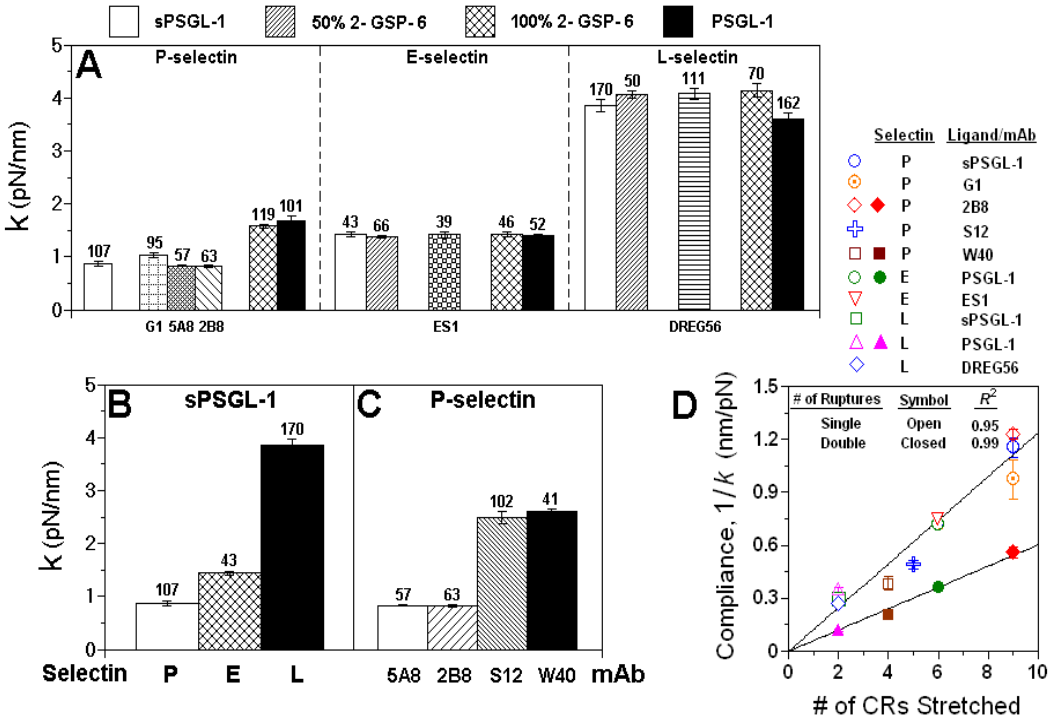

Figure 14: Contribution of Ligand (or Antibody) and CRs to Measured Compliance

The above results were best presented by plotting the molecular compliance ($1/k_m$) against the number of CRs stretched (Figure 14D). For both single as well as double break events, the plots appeared linear, suggesting that the CRs were much more stretchable than not just the Lec/EGF-like domains but also the PEI polymer cushion and the lipid bilayer (Figure 14D). Also, the slope of the linear fit of the single break events was twice that of the double break events, again suggesting that in the double break events, two bonds were being loaded in parallel (Figure 14D). The CRs behaved as

springs in series with a unit elasticity of ~ 8.3 pN/nm, obtained from the inverse of the slope of the linear fit(s) to the data.

4.2 Discussion

The mechanical properties of P-, E- and L-selectins complexed with different ligands and selectin-specific mAbs were characterized using AFM. The use of monomeric and dimeric ligands and different mAbs with different binding epitopes on the selectins helped evaluate the relative contributions of the selectins and the ligands to the complex elasticities (*cf.* Figure 6). Complex compliance was unaffected by changes in ligand while it was directly related to the length of the selectin molecule used (*cf.* Figure 14). The CRs were found to behave as springs in series with a unit elastic constant of ~ 8.3 pN/nm.

The use of elasticity to describe the mechanical property of a selectin assumes that the molecule behaves as a linearly elastic material. To test the validity of this assumption, a large number of *Force vs. Molecular Extension* curves were examined. In the two representative *Force vs. Molecular Extension* curves exemplified in Figure 15, a continuous transition from compressive to tensile forces as z_{pzt} - $\langle z \rangle$ increased is seen in one (Figure 15A), while a dead zone of zero mean force between the compressive and tensile force regimes is seen in the other (Figure 15B). The presence of a dead zone gave the appearance of a non-linear *Force vs. Molecular Extension* relationship. This might have prompted the use of the modified free joint chain (MFJC) model in a previous study, which depicted P-selectin and PSGL-1 as chain-like polymers that required little initial force to straighten their randomly coiled shapes (Fritz et al. 1998). Other studies have

used the free joint chain (FJC) model and the worm-like chain (WLC) model to describe the elastic behaviors of DNA and proteins (Rief et al. 2000). According to these models, a significant part of the elasticity comes from the entropic contribution derived from the random configurations of the contorted polymer.

These polymer elasticity models are given by the following equations:

$$\text{FJC}: \quad z(f) = L[\coth(fl/k_BT) - k_BT/fl]$$
$$\text{WLC}: \quad f(z) = (k_BT/l)\{z/L + 0.25[(1-z/L)^{-2} - 1]\}$$
$$\text{MFJC}: \quad z(f) = (L + f/k\ )[\coth(fl/k_BT) - k_BT/fl]$$

Here L is the contour length, l is the persistence length, and k is an equivalent molecular elasticity. To test the applicability of these nonlinear elastic models to our data, each of the above equations were fit to the measured *Force vs. Molecular Extension* curves (Figure 15A and B).

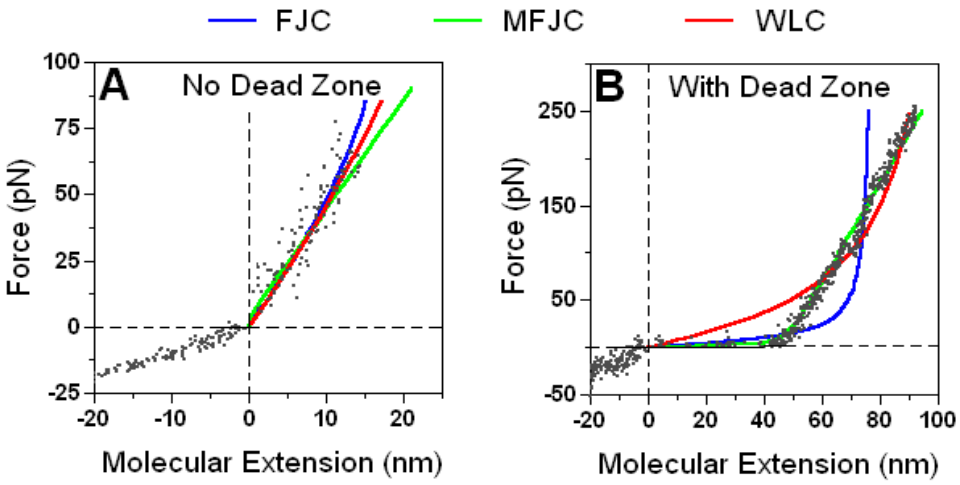

Figure 15: Model Fits for Experimental data without and with Dead Zone

All three models were able to fit curves with no or small dead zones, as these models all have linear regimes that can match the data by adjusting the model parameters (Figure 15A). For curves with much larger dead zones, the WLC model and especially

the FJC model became less and less able to fit the *Force vs. Molecular Extension* curves, as they could not follow the piecewise linear trend of the data no matter how the parameters were adjusted (Figure 15B). The best-fit parameters were found from the fits. The parameter values were L = 2.74 nm, l = 0.77 nm, and k = 4.16 pN/nm for the curve without dead zone (Figure 15A) but L = 47.6 nm, l = 4.79 nm, and k = 5.29 pN/nm for the curve with a ~ 40 nm dead zone (Figure 15B). Moreover, no correlations were found between the k values and the slopes of the linear tensile *Force vs. Molecular Extension* curves, between the L values and the total resting lengths of the molecular complexes or between the l values and any characteristic lengths from the structures of these molecules. Furthermore, although it strongly affected the best-fit parameters, the dead zone length did not correlate with the slope of the tensile *Force vs. Molecular Extension* curve. By contrast, similar slopes (which were taken as molecular elasticities) were observed regardless of the absence or presence of a dead zone.

Collectively, our data supported a linear relationship between applied force and molecular extension, with elasticity primarily due to internal energy. Although the other models were still capable of fitting the *Force vs. Molecular Extension* data, it did not describe the underlying physics of the system, especially that the selectins and PSGL-1 have been shown to be rigid molecules that would not present the entropic elasticity associated with unwinding a polymer.

To further confirm the irrelevance of the polymer elasticity models, the respective local elasticities at a given force (or molecular extension) level for the three models were calculated from the set of equations given above, by differentiating the force with respect to molecular extension and fit to the *Elasticity vs. Force* data (Figure 16).

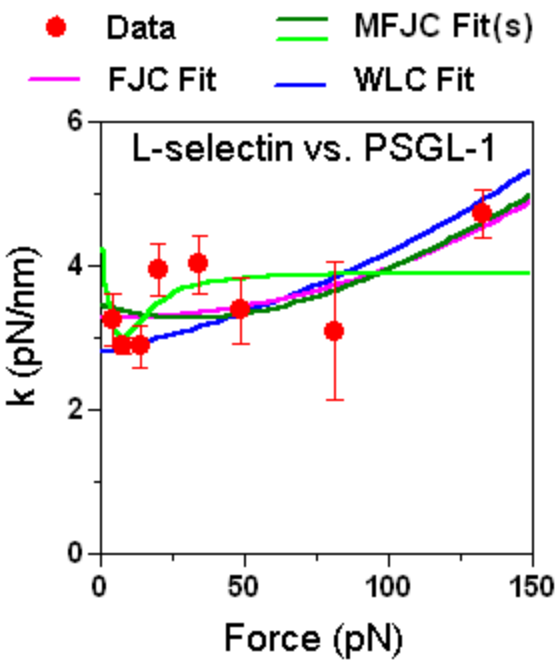

Figure 16: Model Fits for Elasticity vs. Force Data

From the fits, it was evident that the best fits were no better than a linear elastic model with the same elasticity across the entire force range tested. In addition, these fits appeared somewhat arbitrary. For example, two MFJC model fits of nearly identical goodness-of-fits (χ^2 = 1.8 vs. 1.9) had quite different shapes and parameters (L = 50.3 nm, l = 0.01 nm, and k = 1.76 pN/nm vs. L = 2.86 nm, l = 0.88 nm, and k = 3.9 pN/nm) (Figure 16). Thus, aside from its ability to fit the data by freely adjusting its parameters, the MFJC model proposed for the elasticity in the previous study (Fritz, Katopodis et al. 1998) is not justified. Furthermore, the previous study used biotinylated P-selectin-Ig and PSGL-1-Ig chimeras (where the antibody alone on average was modified with 10 biotins) to immobilize the molecules on the coverslips and on the AFM tips (Fritz et al. 1998). This most likely resulted in random length in the specimens that were stretched. Both the invalid model and the poor experimental protocol may have contributed to the inaccurate P-selectin elasticity of 5.3 ± 1.5 pN/nm (Fritz et al. 1998). By comparison, we used

bilayer and capture protocols for immobilizing the selectins and ligands (or mAbs) to ensure uniformity (*cf.* Fig. 3B). While it is still possible for the (s)PSGL-1 captured on the AFM tip to have variable angular rotations, they would most likely result only in small errors because the non-coaxial effect would primarily manifest as variable dead zone lengths. Taken together, our results suggested that the selectins could be modeled as linear springs.

The concept of using the dead zone lengths to predict molecular complex lengths (and hence, individual molecular lengths) is fairly straightforward and does not involve any *a priori* assumption. Hence, it could be extended to other molecular systems, bearing in mind that for different molecular systems, different calibration curves might be needed. From the calibration curves obtained (*cf.* Figure 8), the complex lengths of P- and L-selectins complexed with Endoglycan, a newly identified selectin ligand was obtained. From this, the resting length of (Ig-) Endoglycan was calculated to be ~ 49 nm.

Based on the measured elasticities, a physiological force of ~ 40 pN would result in a ~ 50 nm, ~ 30 nm and ~ 10 nm elongation for P-, E- and L-selectin in that order, which would correspond to a ~ 100 % stretch for each of the selectins. The current AFM data suggested that the selectins elongated but the CRs did not unfold even at these high strains. By comparison, when tested using AFM in similar experiments, titin molecules were found to reversibly unfold at ~ 30 % of stretch (Kellermayer et al. 1997; Rief et al. 1997; Rief et al. 1998). The CR sequences have six identified cysteine residues (Johnston et al. 1989). Alignment with the homologous complement-binding proteins with solved crystal structures suggests that there may be three disulfide bonds in each CR. This would

greatly stabilize its structure, thereby preventing it from being unfolded even under high strains.

Previous studies have shown that neutrophil microvilli can be modeled as springs with an elastic constant of 43 pN/μm, implying that they are ~ 100-folds softer than the selectins (Shao et al. 1998). The microvilli together with the selectins would represent a coupled system, the loading rate profiles of which would be governed by the softer component (microvilli in this case). Computational models for cell adhesion predict lower adhesiveness with increasing elasticities of the linkages (Chang et al. 2000). Thus, selectin-ligand bonds, though stretched by very high forces, would be loaded slowly due to the cushioning effect of the microvilli, thereby decelerating bond dissociation. This could be a possible reason why selectin-ligand bonds are able to link cells under mechanically stressful conditions and capture leukocytes from the blood stream during an inflammatory response.

CHAPTER 5

SPECIFIC AIM #2: DISSECTING THE BOND LIFETIME-FORCE RELATIONSHIP OF L-SELECTIN INTERACTIONS WITH PSGL-1, sPSGL-1, ENDOGLYCAN AND DREG56

Selectin-ligand interactions are rapid and transient. In addition, the mechanically stressful environment in the circulation imposes forces on selectin-ligand bonds, which affect their kinetics. Bell suggested that applied force could accelerate bond dissociation, because work done by the force could lower the energy barrier between the bound and free states (Bell 1978). Conversely, Dembo et al. envisioned that force could also decelerate bond dissociation by deforming the molecules such that they locked more tightly (Dembo et al. 1988). These two types of behavior are named slip and catch bonds, respectively (Figure 17). Since the first experimental determination of the relationship between force and off-rate (Alon et al. 1995), many studies have found slip bond behavior. Counter-intuitive catch bonds were only recently observed for interactions of P-selectin with (s)PSGL-1 in a force range below those previously measured (Marshall et al. 2003).

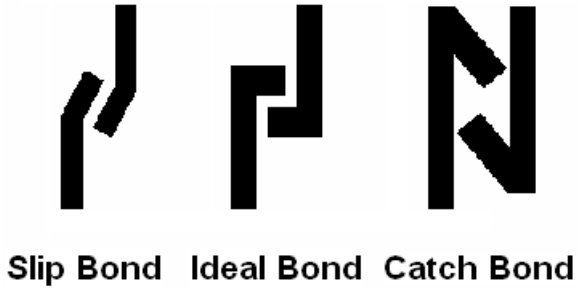

Figure 17: Cartoon Depictions of Different Bond Types

Both P- and L-selectin bind to an N-terminal region of PSGL-1 that must be modified with tyrosine sulfates and an appropriately oriented, sialylated and fucosylated O-glycan (Ramachandran et al. 1999; McEver 2002). Monoclonal antibodies (mAbs) to this region block binding of PSGL-1 to both P- and L-selectin (Moore et al. 1995; Snapp et al. 1998). Compared to P-selectin, L-selectin binds to PSGL-1 with lower affinity and more rapid dissociation kinetics (Alon et al. 1998; Ramachandran et al. 1999). However, the general binding similarities suggested that the L-selectin-PSGL-1 interaction, like the P-selectin-PSGL-1 interaction, could also behave as catch-slip transitional bonds.

Catch bonds have been suggested to partly explain the shear threshold requirement for selectin-mediated adhesion (Marshall et al. 2003): Below the threshold, fewer cells roll and those that do roll less stably and with higher velocities (Finger et al. 1996). Bond lifetimes at low wall shear stresses might be too brief to support stable rolling. As the wall shear stress is increased, catch bonds might retard dissociation at the trailing edge, thereby stabilizing rolling, increasing the number of rolling cells, and lowering their velocities. Compared to that for P-selectin, the shear threshold of L-selectin-mediated leukocyte rolling is much more pronounced and occurs over a much wider range of wall shear stress (Finger et al. 1996; Lawrence et al. 1997). If catch bonds were to contribute to the shear threshold, the L-selectin-PSGL-1 interaction would also behave as catch-slip transitional bonds but with transition over a much wider force range. Endoglycan is a recently identified PSGL-1-like ligand of the CD34 family of sialomucins expressed on endothelial cells (Fieger et al. 2003). Interactions of Endoglycan with L-selectin also support cell rolling under flow. If catch bonds are a general feature of selectin-ligand interactions, the L-selectin-Endoglycan interaction

should also exhibit catch-slip transitional bonds. We tested these hypotheses by using AFM to measure bond lifetimes of L-selectin dissociating from two forms of PSGL-1, from Endoglycan, and from an anti-L-selectin mAb, DREG56.

5.1 Results

5.1.1 Binding Specificity in AFM Experiments

Nonspecific binding was minimized by incorporating L-selectin in a lipid bilayer that was cushioned by a PEI layer, which accommodated inversely oriented molecules (*cf.* Figure 3B and Figure, 18 A-C Open Bars). A substantial increase in binding was seen after functionalizing the tip with (s)PSGL-1 or Endoglycan (solid bars). The binding was specific, because it was abolished by addition of a blocking mAb to L-selectin (DREG56) or to (s)PSGL-1 (PL1) or by addition of the divalent cation chelator EDTA (hatched bars) to the media. In addition, function was restored by replacing the EDTA-containing medium with the normal Ca^{2+}-containing medium (stippled bars). The data shown in panels A, B and C is the cumulative result of 3 different bilayer-tip pairs. 100 adhesion attempts for each pair were carried out. Data are presented as Mean ± S.E.M. DREG56-coated tips also interacted specifically with L-selectin, as demonstrated by their much higher adhesion frequencies than tips adsorbed with anti-PSGL-1 mAb PL2, BSA, or Protein G (Figure 18D).

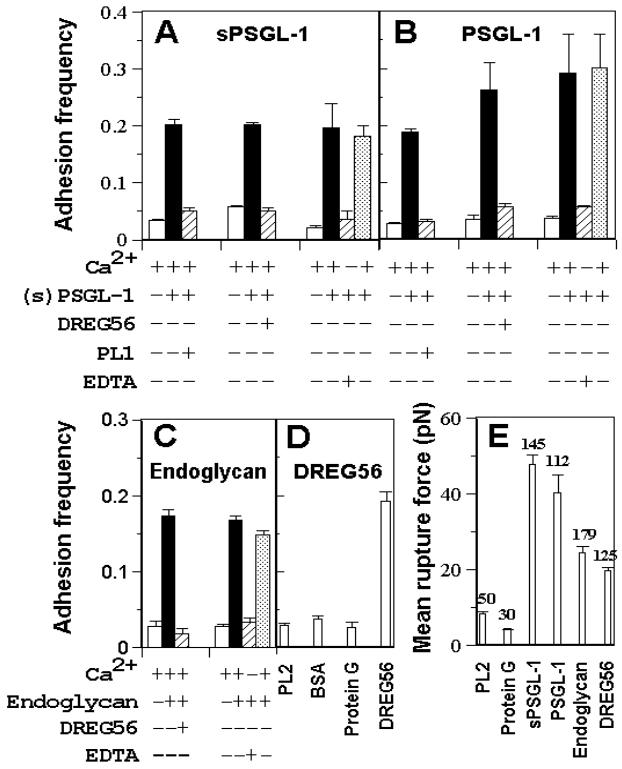

Figure 18: Binding Specificity in AFM Lifetime Experiments

Cantilevers (4-30 pN/nm), coated with (s)PSGL-1, Endoglycan or DREG56 were retracted at 250 nm/s, which corresponded to an approximate bond loading rate of 1000 pN/s. In all lifetime experiments, the L-selectin bilayers were always tested first with yet-to-be ligand-functionalized or BSA-coated tips to confirm the low nonspecific binding. After functionalizing with ligand or replacing the BSA-coated tips with DREG56-coated ones, the experiments were continued to confirm the substantial increase in adhesion frequencies. This ensured that most of the lifetimes measured represented specific interactions of L-selectin with ligand or DREG56. However, the much less frequent nonspecific binding (< 5 %) could have contributed disproportionately long lifetimes and this could have skewed the distribution. To rule out this possibility, the rupture forces of tips functionalized with or without ligand or DREG56 were compared (Figure 18E).

Rupture forces between the L-selectin-bilayers and tips coated only with PL2 or Protein G were exponentially distributed with a mean of ~ 8 or 4 pN. By comparison, much higher mean forces (and hence much longer survival times during the ramping phase when force was increased) were required to detach tips coated with ligand or DREG56 from the L-selectin-bilayers. The rupture force histograms were also qualitatively distinct, exhibiting a bell shape. These data confirmed that the measured lifetimes represented specific interactions.

5.1.2 Catch-Slip Transitional Bonds

To determine if catch bonds existed at force ranges below those previously studied, lifetimes measures at forces as low as 5 pN were obtained, using force averaging to circumvent thermally-driven force fluctuations (Figure 4C and D). As described in the *Materials and Methods* section, lifetime measurements were sorted into force bins and their distribution at each force bin was analyzed by the *Ln(# of events with a lifetime ≥ t) vs. t plot* (Figure 19). The majority of the data (open symbols) followed a straight line, in agreement with the first-order dissociation kinetics of single bonds, which predicts exponential distribution of lifetimes that is linearized by the semi-log plot. A small fraction (≤ 10 %) of the longest lifetimes at some forces significantly deviated from the straight line (color-matched closed symbols), which were judged as outliers and excluded from further analysis.

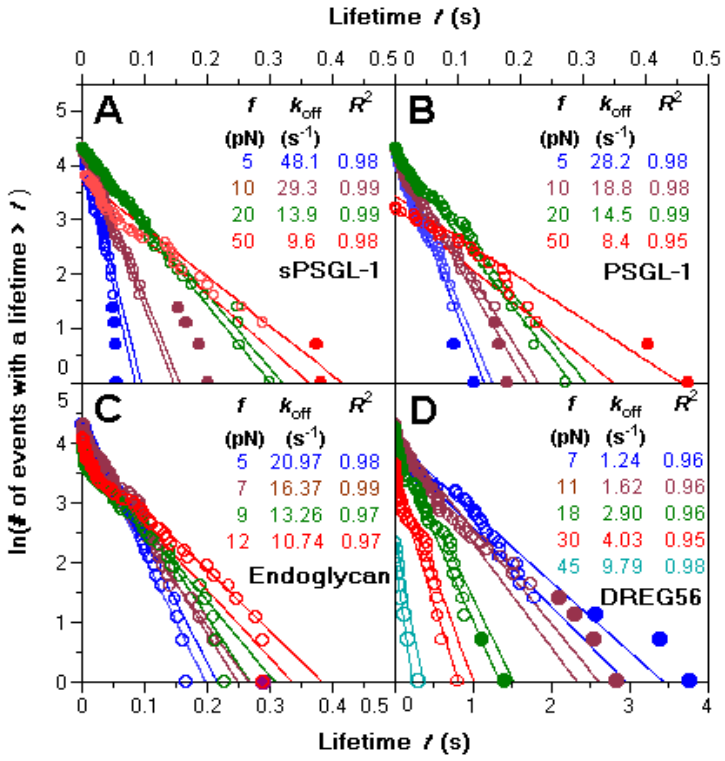

Figure 19: Lifetime Analysis for Single-step Dissociation Events

The lifetime at a given force was estimated from the inverse of the negative slope of the linear fit to the *Ln(# of events with a lifetime ≥ t) vs. t* data and plotted against force (Figure 20). It was also estimated from the mean, $\langle t \rangle$ and standard deviation, $\sigma(t)$ of lifetimes, as per the first-order dissociation kinetics model prediction. Compared to the lifetime distribution, the mean and standard deviation required less data to become statistically stable. This allowed the force dependence of bond lifetime to be examined at finer force bins. As expected, the $\langle t \rangle$ and $\sigma(t)$ data agreed well with the – 1/slope data (Figure 20), which imparted confidence in the lifetime estimates. Similar to the P-selectin-(s)PSGL-1 interactions studied previously (Marshall et al. 2003), the *Lifetime vs. Force* curves of the L-selectin-(s)PSGL-1 and -Endoglycan interactions displayed

biphasic catch-slip transitional bonds. At low forces, the lifetime increased with increasing force, whereas at high forces it decreased with increasing force (Figures 19 and 20: A-C). The error bars represent 95 % confidence intervals of the – 1/slopes of the linear fits to the data (*cf.* Figure 19). Except for a few cases where the differences in the forces were too small, the differences in the lifetime values in the catch bond regime were statistically significant ($P < 0.05$) as determined by the F-test and confirmed by the lack of overlaps in the confidence intervals.

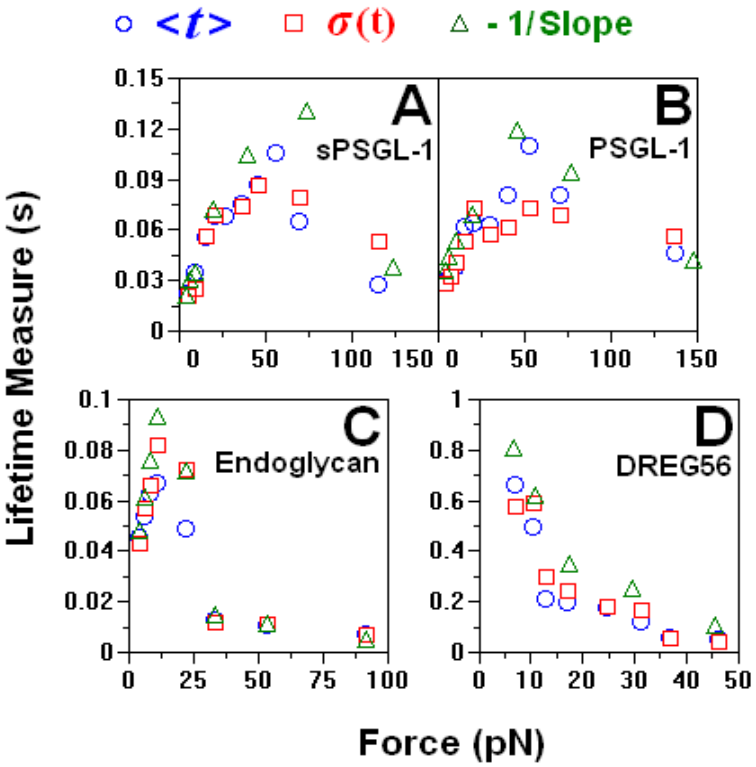

Figure 20: Lifetime vs. Force Plots

Previous studies have revealed that native dimeric PSGL-1 forms dimeric bonds with dimeric P-selectin, which doubled the lifetime and force relative to the interaction between monomeric sPSGL-1 and P-selectin (Marshall et al. 2003). By comparison, the *Lifetime vs. Force* curve of the L-selectin-sPSGL-1 interaction (Figure 20A) was

indistinguishable from that of the L-selectin-PSGL-1 interaction (Figure 20B). These data indicated that, although purified in a similar manner and incorporated in the lipid bilayer in the same way as membrane P-selectin, membrane L-selectin was unable to form dimeric bonds with PSGL-1 as P-selectin did, suggesting that L-selectin behaved as a monomer under the conditions tested. This was again consistent with previously obtained elasticity measurements. Although sharing a qualitatively similar catch-slip transitional bond, the L-selectin-Endoglycan interaction exhibited quantitative differences: The catch bond occurred at 5-15 pN (Figure 20C), a much narrower force range than the L-selectin-(s)PSGL-1 catch bond (Figure 20A and B). After transition to the slip bond regime, the lifetime of the L-selectin-Endoglycan interaction rapidly decreased with force, much faster than the decrease in lifetime of the L-selectin-(s)PSGL-1 slip bond in response to increasing forces (Figure 20 A-C). To examine whether the catch-slip bonds were specific to L-selectin-ligand interactions, the lifetimes of L-selectin dissociating from DREG56 were measured. The lifetime estimated from all three methods decreased monotonically with increasing force (Figure 20D). This slip bond behavior is typical of antibody-antigen interactions (Marshall et al. 2003) and contrasted sharply with the catch-slip transitional bonds of L-selectin with its physiological ligands.

5.2 Discussion

5.2.1 Comparison with Previous Results

Previous experiments with flow chambers have shown that the off-rates of L-selectin interactions with PSGL-1 or with mucin ligands derived from lymph node endothelial cells increased with increasing wall shear stress, behaving as slip bonds (Alon et al. 1997; Alon et al. 1998; Lawrence 1999; Ramachandran et al. 1999). These

experiments were conducted at wall shear stresses that corresponded to tether forces > 40 pN. The present work revealed that L-selectin-(s)PSGL-1 interactions behaved as catch bonds at forces < 50 pN, thus, extending previous results to a lower force range. At higher forces the L-selectin-(s)PSGL-1 interactions behaved as slip bonds, in agreement with previous results. These catch-slip transitional bonds were qualitatively similar to those observed for interactions of P-selectin with (s)PSGL-1 (Marshall et al. 2003), consistent with the structural and functional similarities of L- and P-selectin. The force dependence of lifetime of Endoglycan, a novel L-selectin ligand (Fieger et al. 2003) whose kinetics had not been previously characterized, also behaved as catch-slip transitional bonds. These data suggested that catch-slip transitional bonds could be a common characteristic of selectin-ligand interactions. Catch-slip transitional bonds are detected under conditions in which force was rapidly increased and then became constant, as in the experiments reported here. These conditions resemble those that occur in the circulation and are thus likely to be physiologically relevant.

5.2.2 Evidence for Monomeric Interactions

P-selectin and PSGL-1 both form cell-surface dimers (Barkalow et al. 2000; Epperson et al. 2000) which enhances adhesion under flow (Ramachandran et al. 2001). They remain as stable dimers after purification in nonionic detergents (Ushiyama et al. 1993). By comparison, it is not known whether L-selectin exists as a monomer or oligomer in the cell membrane or in solution. Should our AFM data reflect oligomeric interactions, fitting them with a monomeric binding model would have estimated apparent rather than intrinsic off-rates (off-rate being the inverse of lifetime). It should be noted that even oligomeric binding would not have negated the catch bond observation

in the AFM experiments. To measure lifetimes at a higher force would require a longer time to ramp the force to a higher level before clamping it constant to start lifetime measurements. Should some of the bonds in an oligomeric bond cluster break during ramping, more such rupture events would have occurred at higher forces, yielding oligomeric bonds of lower valency. This would have resulted in shorter lifetimes at higher forces than at lower forces, namely, slip bonds. On the contrary, we observed longer lifetimes at higher forces than at lower forces, namely, catch bonds.

In previous AFM and flow chamber experiments, we observed a rightward and upward shift of the Lifetime vs. Force curve of P-selectin-PSGL-1 interaction relative to that of the P-selectin-sPSGL-1 interaction, approximately doubling the force and lifetime. This demonstrated that P-selectin formed dimeric bonds with PSGL-1 but monomeric bonds with sPSGL-1 (Marshall et al. 2003). Thus, purified P-selectin remained dimeric after being reconstituted into glass-supported lipid bilayers, and purified PSGL-1 remained dimeric after being captured on the AFM tips by mAb PL2. The present AFM experiments were performed under identical conditions, except that purified L-selectin was used *in lieu* of purified P-selectin. However, the *Lifetime vs. Force* curves were indistinguishable for interactions of L-selectin with PSGL-1 or sPSGL-1, suggesting that monomeric bonds were measured in both cases (*cf.* Figure 20A and B). The above observation have been further bolstered by molecular elasticity measurements, which revealed the same elasticity for L-selectin complexed with either form of PSGL-1 (*cf.* Fig. 10B), while P-selectin-PSGL-1 elasticity was twice that of the P-selectin-sPSGL-1 complex (*cf.* Fig. 10B).

5.2.3 Catch Bonds and Shear Threshold Phenomenon

The counter-intuitive shear threshold requirement for selectin-mediated leukocyte adhesion had not been satisfactorily explained, till recently. Chen and Springer showed that the average number of tether bonds calculated from pause times of L- and E-selectin-mediated neutrophil rolling decreased with decreasing wall shear stress, which extrapolated to a value < 1 at wall shear stresses too low to support rolling (Chen and Springer 1999). The authors hypothesized that a minimum shear was required to rotate the cells sufficiently fast to allow the interacting molecules to penetrate the repulsive barrier to enable binding. Chang and Hammer modeled cell binding under flow as a two-step process: (1) A transport step, in which molecules are carried by the moving cell to the vicinity of counter-molecules immobilized on a surface and (2) A reaction step in which the interacting molecules dock (Chang and Hammer 1999). The authors suggested that a minimum shear was required for transport to enhance the overall on-rate to support rolling. Cell deformation has also been suggested to contribute to the shear threshold. The hydrodynamic drag exerted on a rolling cell has to be balanced not only by the tensile force acting on the tethers at the cell rear but also by the compressive force acting on the cell front, which might flatten the cell membrane locally, thereby enlarging the contact area and enhancing new bond formation (Lawrence et al. 1997; Evans 2001; Zhao et al. 2001). These hypotheses attribute on-rate as responsible for the shear threshold. It could be possible that catch bonds – an off-rate characteristic – could contribute to the shear threshold. At low shear, bonds dissociate too rapidly to support rolling; increasing shear decelerates bond dissociation, thereby stabilizing rolling (Marshall et al. 2003).

The shear threshold requirement is much more pronounced for rolling mediated by L-selectin than by P- or E-selectin (Finger et al. 1996; Alon et al. 1997; Lawrence et

al. 1997). L-selectin-(s)PSGL-1 interactions behave as catch bonds at low forces that coincide with sub-threshold wall shear stresses (Figure 18A and B) wherein the number of L-selectin-mediated rolling cells increase and their velocities decrease with increasing shear. The force range for P-selectin catch bonds is much lower, consistent with the much more modest shear threshold for P-selectin-mediated rolling (Lawrence et al. 1997; Marshall et al. 2003). These combined data support the potential physiological relevance of catch-slip bond transitions for rolling adhesion mediated by each selectin. Very recently, this paradox has been solved in an elegant manner, wherein catch bonds were shown to be the causal factor for shear threshold phenomenon (Yago et al. 2004).

5.2.4 Effect of Serial Linkages on Force vs. Lifetime Curves

In the lifetime experiments discussed, (s)PSGL-1 was captured using PL2 while Ig-Endoglycan was captured using Protein G. Both PL2 and Protein G were in turn physi-adsorbed on the AFM cantilever tips. It may be recalled that slip bonds in the L-selectin-Endoglycan interactions set in at a much lower force regime than the (s)PSGL-1 interactions (Figure 20 A-C). This could be possible if the Protein G-Ig-Endoglycan link were to snap off even before L-selectin were to dissociate from Ig-Endoglycan. In order to address this issue, experiments were performed wherein Ig-L-selectin was captured on the AFM tip using Protein G and a membrane form of PSGL-1 was incorporated in the bilayer. In essence, the orientation of the molecular system (involved in generating Figure 20B data) was reversed. As such, if the orientation of the system and the Protein G-capturing of Ig-Endoglycan on the AFM tip had to have no effect, then the *Lifetime vs. Force* curves for this system would have been very similar to the one in Figure 20B. But, this was not the case (*cf.* Figure 20B and Figure 21). For the inverted system, while the

lifetimes were very similar, the catch-slip transitions occurred over a narrower force range (Figure 21), which could be possible if dissociation of the Protein G-Ig-Endoglycan linkage would have occurred. If one were to view the Protein G-Ig-Endoglycan and the Ig-Endoglycan-L-selectin bonds in series, then, the apparent off-rate of the system would be the sum of the individual off-rates. This could be a potential reason why there are visible differences between the data in Figures 18A and 21. However, the key thing to note is that from a qualitative standpoint, the catch-slip transitional bonds are common for L-selectin-(s)PSGL-1 as well as L-selectin–Endoglycan interactions.

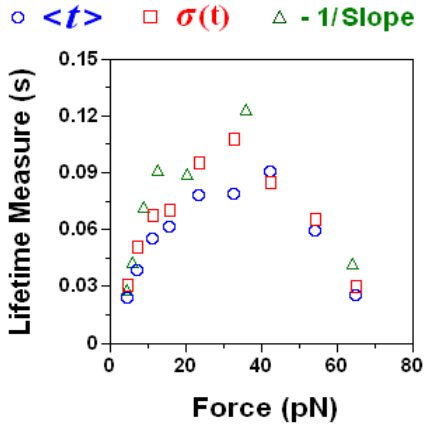

Figure 21: Lifetime vs. Force Curve for Inverted System

5.2.5 Models for Catch-Slip Transitional Bonds

The concept of catch bonds originated as an off-shoot of a mathematical expression for force dependence of off-rate (Dembo et al. 1988). To provide a physical picture for this theoretical possibility, the authors proposed a geometrical model – a finger-prison in which applied force deformed the molecules such that they locked

together more tightly (*cf.* Figure 17). At least two other physical mechanisms can be envisioned for the catch-slip transitional bond, which cannot be explained by the finger-prison model.

One possible mechanism for catch-slip transitional bonds, is a *Two-Pathway Model* that will be discussed in Chapter 6 (*cf.* Figure 27) (Evans et al. 2004; Sarangapani et al. 2004). The other model, namely the *Differential Destabilization Pathway Model* stems from the chemical principle that off-rate is inversely proportional to the exponential of the height of the energy barrier to dissociation, i.e., the difference in binding energy between the transition state and the bound state, scaled by the thermal energy (Figure 22A). Applied force tends to destabilize the bound state by raising its energy, which, for simplicity, is assumed to increase linearly with force (Figure 22B). Suppose that the applied force also destabilizes the transition state (Figure 22B) but raises its energy at a rate that is at first faster and then slower than the rate at which the bound state energy increases with increasing force. The resulting energy barrier height would then, first increase and decrease with force, resulting in a catch-slip transitional bond (Figure 22A and B).

This model is an extension of the model proposed by Dembo et al. (Dembo et al. 1988). The different shapes of the *Energy vs. Force* curves for the bound and transition states would provide a mechanism for changing from catch to slip bonds in different force regimes. By comparison, the previous model assumed similarly shaped quadratic functions for the force dependence of both the bound state and the transition state energies, which are represented by two springs with either the same spring constant or the same resting length, which allows only slip, catch, or ideal bonds (Dembo et al. 1988).

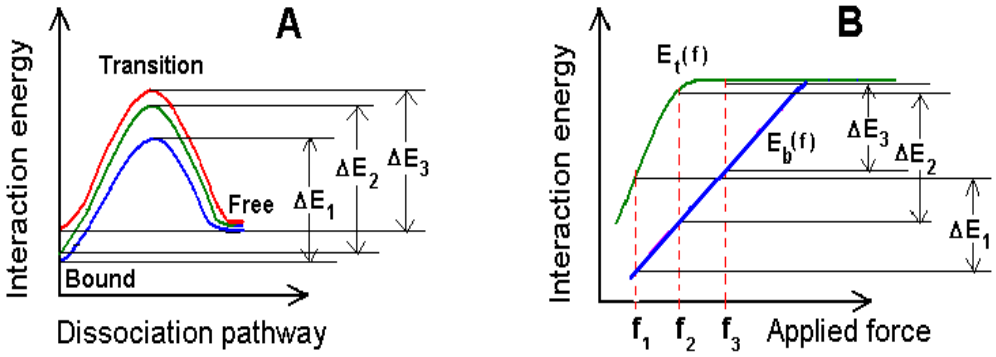

Figure 22: Differential Destabilization Pathway Model

CHAPTER 6

SPECIFIC AIM#3: CHARACTERIZING THE FORCE HISTORY DEPENDENCE OF L-SELECTIN-LIGAND DISSOCIATION

Bell proposed that the relationship between off-rate and force in receptor-ligand dissociation could be modeled based on the isotropic theory of solids in mechanics (Bell 1978). Ever since, this model has served as the gospel in almost all of receptor biomechanics studies. While the Bell model suggests an exponential relationship between off-rate and force, Dembo et al. suggested that force could also do the opposite to the receptor-ligand bond (Dembo et al. 1988). They envisioned a finger-prison model, wherein a force-induced conformational change could decelerate bond dissociation by facilitating more inter-locking of the binding pockets on apposing molecules. Termed catch bonds, till recently, they existed only as a theoretical possibility (Marshall et al. 2003).

Dynamic Force Spectroscopy (DFS) has been heavily employed to map the energy landscape of receptor-ligand unbinding (Evans 1998; Evans 1999; Merkel et al. 1999; Evans 2001). But, off-rates derived from DFS analysis differ substantially from AFM lifetime studies for the same selectin done in our lab in the past (*cf.* Figure 20 and (Evans 2001). This is not an isolated case for L-selectin-mediated interactions. Previously, Marshall et al. tested P-selectin interactions with (s)PSGL-1 and anti-P-selectin mAb G1 and found that the off-rates obtained from AFM lifetime assays were qualitatively and quantitatively different from previously published P-selectin studies as well as from DFS analysis of the data obtained from AFM unbinding force assay using the same batch of reagents (Marshall et al. 2005). This was puzzling because all other

things being constant, the only variable between the two assays were the assays themselves. While one was a ramp force assay, wherein the bond was loaded till rupture, the other was the ramp and hold assay, which has been adopted in specific aim # 2 of this work. Off-rate is an intrinsic property that depends solely on the molecules involved, and as such, should not depend much on the type of assay adopted in quantifying it. If not for the quantitative differences, it was the qualitative differences that kick-started the concept of force history. While the lifetime assay showed counter-intuitive catch-slip transitional bonds which was independently confirmed by flow chamber measurements (Marshall et al. 2003), the unbinding force assay predicted the more intuitive slip bonds, wherein bond lifetimes dropped precipitously with applied force (Marshall et al. 2005).

Careful analyses suggested that the *a priori* assumption in the DFS analysis could be false and that this could be the cause of the apparent discrepancy. Besides, in the lifetime assay data analysis, the rupture events that did not survive the PZT motion (i.e. the ramp phase) were excluded and only those events that survived the PZT motion were considered. This in effect, could amount to selecting a stronger, longer-lived subpopulation of bonds. In order to address this issue, the data from the two different assays were analyzed by a newly-developed time-to-rupture analysis and the off-rates were expressed as a function of bond survival time, along a specified history of force application. The advantage of this analysis was that besides taking into account all events (i.e. no data biasing) the assay did not assume any model for the forced dissociation of the molecular complex. Amazingly, when the data from the two different assays were analyzed on such a common platform, the discrepancies resolved (Marshall et al. 2005). This suggested that off-rate was not just dependent on the force but on the entire history

of force application. Hence, the proposed relationship between off-rate and applied force as suggested by Bell (Bell 1978) could not always be true. In this way, the concept of force history dependence of off-rate was conceived.

The concept of force history appears more deep-seated than the Bell model because the latter would be a special case of the former, if one were to consider bond(s) subjected to constant force(s) only. But, physiologically, the selectin-ligand bonds form and break under flowing conditions and there is a phase wherein the bonds are loaded to the force level, determined by the shear. Hence, it is very logical to guess that off-rates would be dependent both on the force and loading rate (or how the force was reached). Though this concept promised to provide a new paradigm to understand how force could regulate bio-molecular interactions, it had not yet been tried and tested for other receptor-ligand systems.

Also, since it challenged a 25-year old paradigm and since it compared data obtained from two different assays, it was increasingly difficult to get the point across without too much of an ambiguity. In order to address this issue, we decided to adopt simpler AFM experimental protocols, whose data interpretation would be fairly straight-forward and relatively easy to understand. L-selectin interactions with monomeric sPSGL-1, a short synthetic PSGL-1 mimic called 2-GSP-6 and a sulfated sugar, 6-sulfo-sLe^x were characterized. L-selectin-sPSGL-1 (and 2-GSP-6) systems were chosen primarily because of the monomeric nature of the interactions (*cf.* Figures 10, 12, 13 and 20). L-selectin-6-sulfo-sLe^x system was chosen as a system control.

6.1 Results

6.1.1 New Experimental Protocol

Membrane L-selectin was incorporated into a glass-supported lipid bilayer cushioned by a polymer (PEI) layer. Monomeric sPSGL-1 and biotinylated 2-GSP-6 and 6-sulfo-sLe^x were respectively captured using anti-PSGL-1 mAb PL2 and streptavidin. Lifetime measurements were performed wherein the sPSGL-1- (or 2-GSP-6- or 6-sulfo-sLe^x-) coated AFM tips where brought into and out of contact with the L-selectin-incorporated lipid bilayers. The *Lifetime vs. Force* relationships were characterized in exactly the same way as in specific aim # 2 (*cf.* Sections *3.7* and *3.10*). The new addition to the existing protocol was that lifetime experiments were performed at different retraction speeds of the cantilever. Thus, *Lifetime vs. Force* curves were obtained at different bond loading rates i.e. along different force-loading paths (indicated by the different colored lines in Figure 23) before reaching pre-determined force levels (f_1, f_2 , f_3 etc).

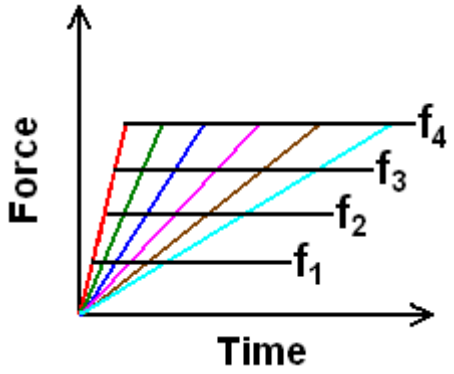

Figure 23: Force History AFM Experimental Protocol

All data were acquired at 3 kHz. For ensuring statistical stability, data were pooled in from many experiments and between 350 and 450 lifetimes were collected, for each bond loading rate, for all molecular systems. Bond loading rates were varied

between 1000 and 100,000 pN/s. In order to minimize the effects of hydrodynamic drag at high bond loading rates, stiff cantilevers of spring constant 100 pN/nm (as prescribed by the manufacturer) were used in most of the experiments. During each experiment, one bilayer-tip pair was used and interactions at 3 different bond loading rates were tested.

6.1.2 Binding Specificity in Force History Experiments

As in specific aim # 2, it was necessary to demonstrate the specificity of the interactions, to begin with. Nonspecific binding was minimized by incorporating L-selectin in a lipid bilayer that was cushioned by a PEI layer, which accommodated inversely oriented selectin molecules. During each experiment, the bilayer was first tested for nonspecific binding before functionalizing the AFM cantilever tips with sPSGL-1. A substantial increase in binding was seen after functionalizing the tip. The binding was specific, because it was abolished by addition of a blocking mAb to L-selectin (DREG56) or to sPSGL-1 (PL1) or by addition of the divalent cation chelator EDTA to the media (data not shown). In addition, function was restored by replacing the EDTA-containing medium with the normal Ca^{2+}-containing medium. 150 adhesion attempts for each pair were carried out. Two such cantilever tip-bilayer pairs were tested. Likewise, binding specificity experiments for tips coated with 2-GSP-6 and 6-sulfo-sLex were also performed (data not shown).

Experiments were performed by repeatedly bringing the ligand-coated cantilevers into and out of contact with the L-selectin bilayers. In order to ensure that majority of the adhesion events represented single bonds instead of a cluster of bonds, binding frequency was kept to a minimum (~ 15 -20 %). On a few occasions, double breaks that represented

double bonds were observed. Very rarely were triple rupture events seen. Rupture events with 4 or more breaks were never recorded. The distributions of null, single, double etc rupture events were analyzed and it was found that the distribution fit a Poisson distribution model very well, in accordance to small number statistics (Figure 24). Very similar model parameters were found to satisfy experimental data from each individual experiment as well as the overall cumulative data (of all experiments) (data not shown). The plot shown in Figure 24 is the cumulative result of 4 experiments, with 300-500 adhesion attempts in each experiment. The error bars represent STD of measurements.

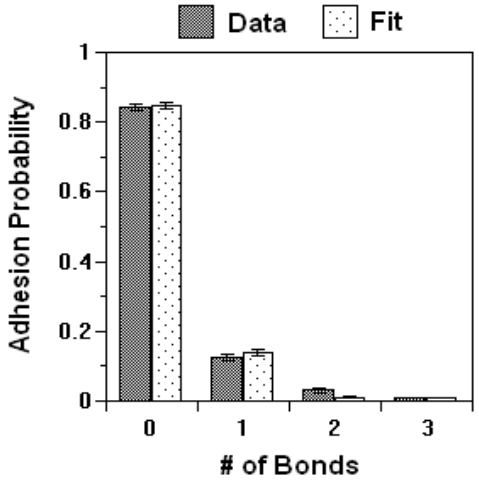

Figure 24: Poisson Model Fit to Adhesion Frequency Data

6.1.3 Loading Rate Sensitivity of L-selectin-sPSGL-1 Interactions

Bond lifetimes measurements were started after the PZT stopped moving (*cf.* Figure 4C and D). Bond lifetime at a given force was calculated using three independent methods as previously described (*cf. 3.7 & 3.10* and Figures 19 & 20). Force history suggests that off-rates of receptor-ligand bonds would not just depend on the force value (hold phase after the PZT stopped moving) but also on the bond loading rate (ramp phase

when the PZT was in motion). Equivalently, bond lifetime (which is the inverse of off-rate) at a given force level would depend not only on the force value but also on the path of force application. In thermodynamics, state functions like enthalpy and entropy depend on the initial and final states of the system. The net change in the enthalpy or entropy, while going from state 1 to state 2, would depend only on the initial (1) and final (2) states of the system and not on the path traversed. Thus, if Bell model (Bell 1978) were to be totally infallible and the concept of force history for P-selectin was an isolated example (Marshall et al. 2005), the L-selectin-sPSGL-1 bond lifetimes could be likened to the state functions and would not be affected by what happened before the PZT stoppage. One would then expect the *Lifetime vs. Force* curves of the L-selectin-sPSGL-1 interactions to be insensitive to the bond loading rates (i.e. to the paths). To put this hypothesis to test, experiments were performed by repeatedly bringing the sPSGL-1-coated AFM cantilever tips into and out of contact with L-selectin-incorporated lipid bilayers and lifetime measurements at different bond loading rates were carried out. Bond loading rates were varied by altering the retraction speeds of the cantilever. However, care was taken to minimize and if possible, totally avoid any hydrodynamic drag effects. During each experiment, lifetime measurements were performed at three distinct bond loading rates using the same bilayer-tip pair.

Lifetime experiments were first performed at a bond loading rate of 1000 pN/s, which was in essence, a repeat of the specific aim # 2 experiments involving L-selectin and sPSGL-1 (*cf.* Figure 20A). However, the results of aim # 2 were obtained using cantilevers whose spring constants ranged between 4 and 30 pN/nm. In the force history experiments, stiffer cantilevers whose spring constants were 100 (±20) pN/nm were used

in most of the experiments. The main idea to use stiff cantilevers was to reduce the hydrodynamic effects at high retraction speeds of the cantilevers. Using stiff cantilevers however posed some constraints on the force resolution, especially at very low forces. This problem was overcome by obtaining data at a high scan rate (3 kHz) and using a force-averaging protocol to circumvent thermally-driven force fluctuations (Marshall et al. 2003) (*cf.* Figure 4C and D).

It should be expected that the measured properties, be it kinetic or mechanical, should not be biased or influenced by parameters like the cantilever stiffness and size. In fact, the elasticity measures of P- and L-selectins complexed with different ligands and mAbs were found to be independent of the AFM cantilever shape and size (Marshall et al., *Biophys. J.* in review). Consistent with these observations, the new *Lifetime vs. Force* data was in excellent agreement with the previously obtained data (*cf.* Figure 20A and Figure 25A). Besides, the harmony in results also bore testimony to the repeatability and reproducibility of our AFM experimental protocols. At a bond loading rate of 1000 pN/s, the *Lifetime vs. Force* curve was biphasic, with catch bonds operating at low forces followed by a transition to slip bonds as the force became higher (Figure 25A). However, as the bond loading rate gradually increased, the *Lifetime vs. Force* curves started showing quantitative ***and*** qualitative differences. As the bond loading rates increased, the catch-slip transition location i.e. the position on the force- (or the x-) axis of lifetime maximum gradually started shifting inwards, towards the lifetime- (or the y-) axis (Figure 25 A-C). Despite this, the peak lifetime value was not dramatically altered. As the bond loading rates became higher and higher, the catch-slip transitional bonds could no longer be clearly deciphered and the *Lifetime vs. Force* curves started exhibiting slip bond

behaviour, with the bond lifetimes precipitously dropping with force (Figure 25 D-F). Amazingly, the *Lifetime vs. Force* curves in Figure 25 – Panels D, E and F could be fit using very similar exponential fitting parameters (data not shown). This indicated that beyond a certain point, the bond loading rate did not have any impact on the nature of the *Lifetime vs. Force* curves. In other words, after exhibiting tremendous sensitivity to loading rates between 1000 and 7000 pN/s, the interactions became insensitive to the bond loading rates at values ≥ 7000 pN/s.

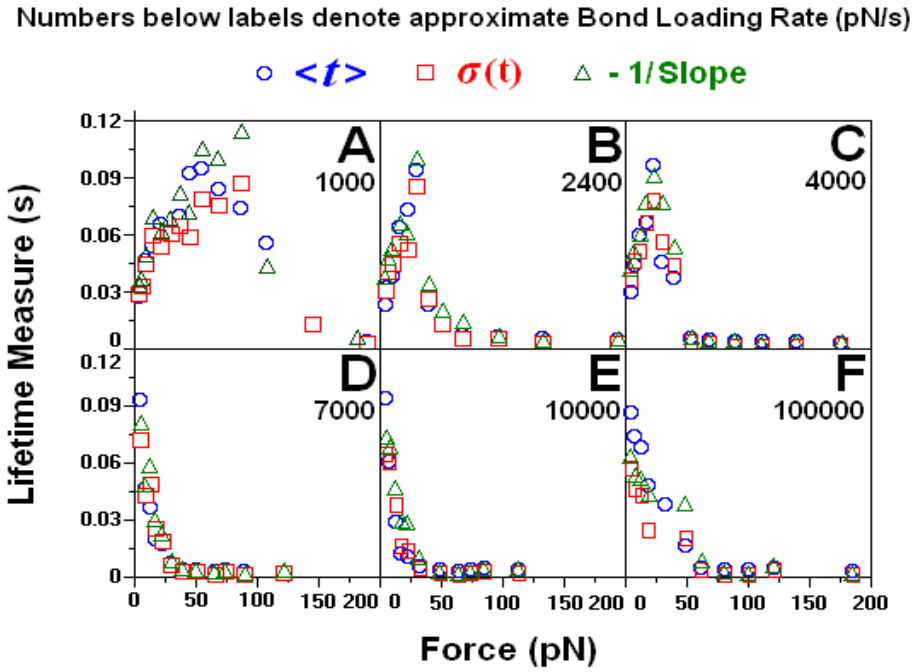

Figure 25: Lifetime vs. Force Curves at Various Bond Loading Rates for sPSGL-1 System

The data presented in Figure 25 (all panels) were performed by the same experimenter using the same AFM set-up and same batch of reagents. Data obtained from many independent experiments were pooled together for ensuring statistical robustness. On a given day, the same bilayer-tip pair was used to carry out lifetime measurements at

three different bond loading rates. It could be safely assumed that the same number and type of bonds would have been formed before the bonds were loaded with force and subsequently tested in the different loading rate cases. In previous studies, Evans et al. have reported an increase in the adhesion frequency with increasing bond loading rate (Evans et al. 2004). However, no such marked increase in adhesion frequency was observed in the current AFM experiments (Figure 26), with the value between 15 and 20 % in all the cases and in accordance to Poisson statistics (*cf.* Figure 24). Yet, the *Lifetime vs. Force* curves had qualitative and quantitative differences between them, at various loading rates (Figure 25). This intense dependence of the *Lifetime vs. Force* curves to the bond loading rate suggested that there could be an element of force history at work, which affected bond lifetimes at a given force, when the force was reached via different paths. Error bars in Figure 26 denote S.E.M.

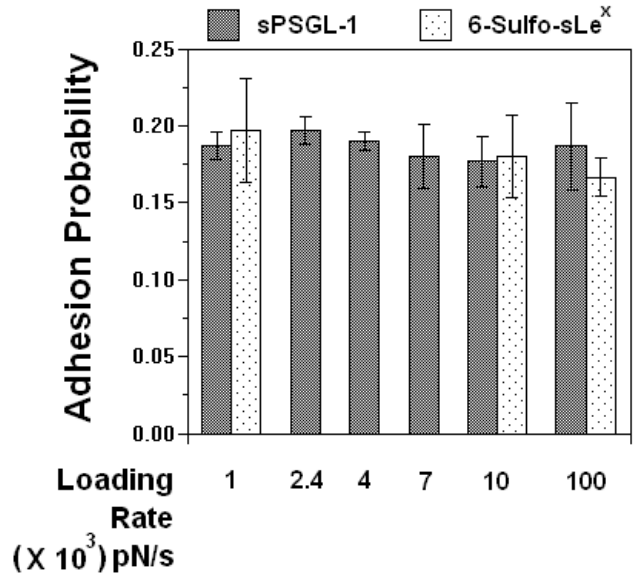

Figure 26: Adhesion Frequencies at Various Bond Loading Rates

6.1.4 Two-Pathway Model and Experiments with Sulfated Sugar Moiety

The biphasic behavior of the curves in Figure 25 A-C can also be explained if one were to think of a *Two-Pathway Model* (Evans et al. 2004; Sarangapani et al. 2004). This mechanism assumes that a bond can dissociate along two *force-sensitive* pathways – one fast and the other slow – with different probabilities (Figure 27A). Suppose that the probability of dissociation along the slow pathway is small at low force but increases with increasing force and the probability of dissociation along the fast pathway is large at low force but decreases with increasing force. Increasing force would first slow dissociation because it is increasingly more likely to take place along the slow pathway (Figure 27B). After the slow pathway becomes predominant, continued increase in force would then accelerate dissociation by suppressing the energy barrier on this pathway (Figure 27C).

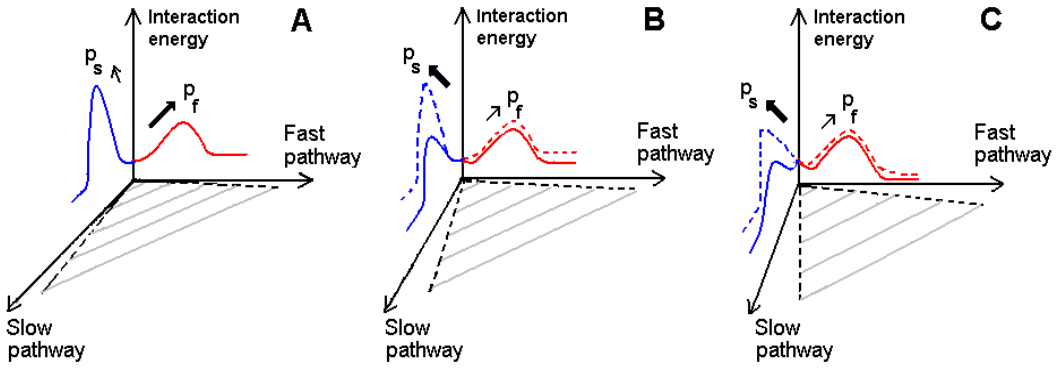

Figure 27: Two-Pathway Model

Evans et al. have suggested that the two distinct pathways could be traced back to the peptide component and the sugar component of the ligand (Evans et al. 2004). Their data suggests that the slow pathway is due to the peptide component and the fast pathway is primarily due to the sugar moiety. When P-selectin was tested against biotinylated sLe^x, only slip bonds were observed (Evans et al. 2004). Hence, according to this model,

if one were to test just a sugar moiety against a selectin, catch-slip transitional bonds would not be observed.

To put this to test, we carried out lifetime experiments at different bond loading rates wherein L-selectin was tested against biotinylated 6-sulfo-sLe^x. Amazingly, unlike the L-selectin-sPSGL-1 interactions, the *Lifetime vs. Force* curves of L-selectin-6-sulfo-sLe^x interactions did not change qualitatively or quantitatively, over a range of bond loading rate spanning two orders of magnitude (Figure 28 All Panels). Furthermore, the curves were biphasic – with a catch bond operating at the low force regime. This strongly suggested that the Evans et al.'s version of the Two-Pathway Model could not satisfactorily explain the loading rate dependence of L-selectin-sPSGL-1 interactions.

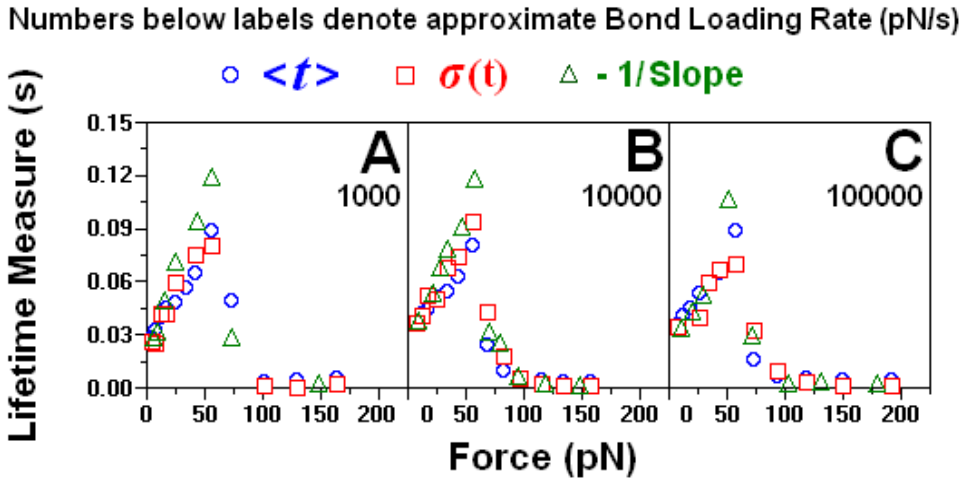

Figure 28: Lifetime vs. Force Curves at Various Bond Loading Rates for 6-Sulfo-sLe^x System

However, the Two-Pathway Model could still be used to explain the data shown in Figure 25 (all panels) but with an additional constraint namely that the selection of the slow or the fast pathway is decided by both the force *as well as* the bond loading rate. At low bond loading rates (below a certain putative threshold), the slow or fast pathways would be decided only by the force level (thus, giving rise to a catch-slip biphasic

behavior) while at bond loading rates above the threshold, the fast pathway would be selectively favored over the slow pathway, giving rise to slip bonds only. With this additional constraint, the Two-Pathway Model becomes a model of Force History because by including the bond loading rate as a parameter, the loading history of the bond would be automatically taken into account. It could be possible that for the 6-Sulfo-sLe^x case, the interactions are dependent only on force and are insensitive to bond loading rate.

6.1.5 Experiments with 2-GSP-6

While the L-selectin-sPSGL-1 bond's response to increasing loading rate interactions differed qualitatively from that of L-selectin-6-sulfo-sLe^x, there was one major difference in the experimental protocol and that was the way in which sPSGL-1 and 6-sulfo-sLe^x were respectively captured on the AFM cantilever tips. While sPSGL-1 was captured using a capture antibody (PL2), 6-sulfo-sLe^x was captured using streptavidin. If one were to argue that biotin-streptavidin linkages are biochemically and mechanically different from a typical antigen-antibody linkage (PL2-sPSGL-1), then, it is possible that this difference in the nature of the mechanical linkages could have impacted the measurements. It could have been possible that during the high loading rate attempts, the PL2-sPSGL-1 link could have snapped off even before sPSGL-1 could dissociate from L-selectin and the data shown in Figure 25 D-F (slip bond behavior) could have resulted due to this factor.

In order to address this issue, L-selectin force history experiments with 2-GSP-6, a short synthetic mimic of PSGL-1 were performed. It has been shown that 2-GSP-6 is good enough to sustain stable interactions with P-selectin (Yago et al. 2002). Recently, flow chamber experiments have been performed wherein 2-GSP-6 was tested against L-selectin.

The *Off-rate vs. Force* curve was biphasic with a catch-slip transitional bond (Yago et al., unpublished data) and the results were qualitatively very similar to previously published L-selectin-sPSGL-1 results (Sarangapani et al. 2004). In the AFM experiments, biotinylated 2-GSP-6 was captured using streptavidin, in exactly the same way biotinylated 6-sulfo-sLe^x was captured. Lifetime measurements at three different bond loading rates (1000, 4000 and 7000 pN/s) were obtained.

Preliminary experiments and data analysis revealed that the *Lifetime vs. Force* curves of the 2-GSP-6 system were qualitatively very similar to those of the sPSGL-1 system at similar bond loading rates (*cf.* Figure 25 A, C & D and Figure 29 A-C). The striking feature was that the lifetime maximum position gradually shifted inward towards the lifetime or y-axis (Figure 29A & B) and catch-slip transitional bonds totally disappeared at 7000 pN/s bond loading rate, very similar to the L-selectin-sPSGL-1 interactions (Figure 29C). This suggested that the bond loading rate dependence of the L-selectin-sPSGL-1 interactions as exemplified in Figure 25 was not due to the PL2-sPSGL-1 linkage snapping off during the pulling phase.

Collectively, all the data suggested that the only plausible explanation for the observed differences in L-selectin-sPSGL-1 (and 2-GSP-6) interactions at different bond loading rates was force history. This new paradigm has thrown up a challenge to the existing Bell model school of thought and will definitely pave way for new ideas and thinking in the field of how force can regulate specifically selectin-ligand and in general, receptor-ligand biology.

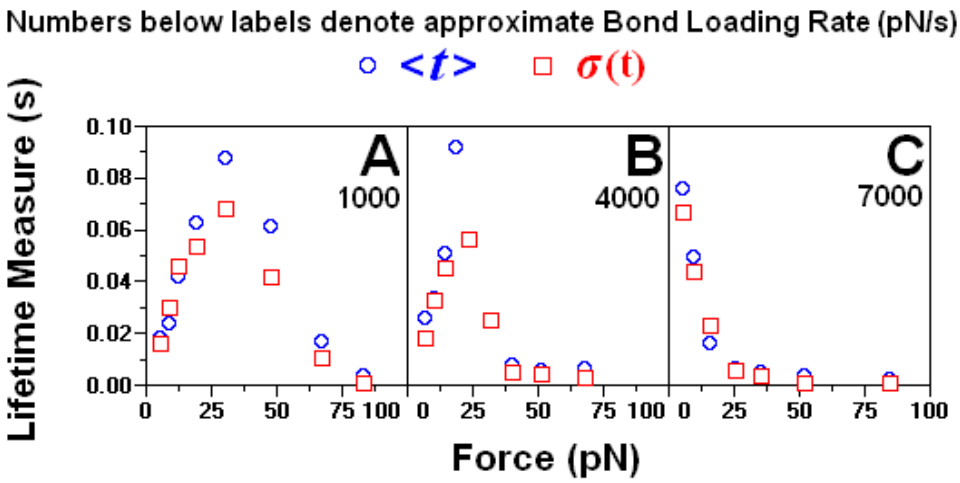

Figure 29: Lifetime vs. Force Curves at Various Bond Loading Rates for 2-GSP-6 System

6.2 Discussion

The concept of force history has challenged a ~ 25-year old paradigm that has till now, been the gospel in forced receptor-ligand dissociation. However, the fact that the L-selectin-sPSGL-1 (and 2-GSP-6) *Lifetime vs. Force* curve is dependent on the bond loading rate suggests that the concept of force history is here to stay. This concept has been previously shown to hold for P-selectin-mediated interactions (Marshall, Sarangapani et al. 2004). Now, by a simpler experimental protocol and unequivocal and straight-forward data analysis and interpretation, we have demonstrated this concept for L-selectin-mediated interactions as well. In the process of zeroing on force history, we have methodically considered and eliminated other possible explanations for this phenomenon.

The loading rate dependence of L-selectin-sPSGL-1 (and 2-GSP-6) interactions can best be summed up by plotting the optimal force (i.e. the force at which lifetime is maximum in the *Lifetime vs. Force* curves) as a function of the bond loading rate (Figure

30). The heavy loading rate dependence of the optimal force for the sPSGL-1 (and 2-GSP-6) interactions can be clearly seen. Especially for the sPSGL-1 case, the optimal force drops precipitously when loading rate is increased. After a certain point (~ 7000 pN/s), the optimal force value is relatively insensitive to increase in bond loading rate. While this is the case for sPSGL-1, for the 6-sulfo-sLe^x interactions, the optimal force is relatively indifferent to the bond loading rate. Though for the 2-GSP-6 interactions, only data at three bond loading rates are available, it is reasonable to guess that data at higher loading rates would follow a trend qualitatively similar to that of sPSGL-1, primarily because of the fact that 2-GSP-6 is in essence, a short synthetic mimic of PSGL-1.

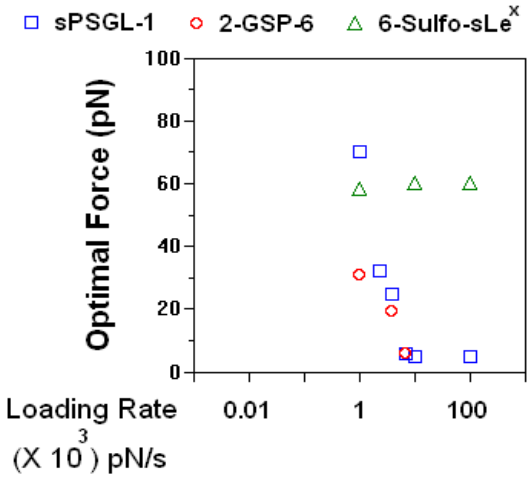

Figure 30: Optimal Force vs. Bond Loading Rate Plot

6.2.1 Static vs. Dynamic Approach to Eliminating Catch-Slip Transitional Bonds

The fact that L-selectin-sPSGL-1 interactions display force history suggests that the previously published P-selectin study is not an isolated example of a system that displays force history behavior (Marshall et al. 2005). In the present study, lifetime measurements did not start until after the force reached a pre-determined value. The fact

that there are qualitative differences between the data in different panels (Figure 25) suggests that the force application prior to lifetime measurement did somehow impact the duration of the bonds. While this was the case with sPSGL-1 (and 2-GSP-6), the *Lifetime vs. Force* curves for L-selectin interacting with a sulfated sugar moiety was insensitive to bond loading rate.

Dr. McEver's lab (OMRF, Oklahoma City, OK) has designed and produced a mutant form of L-selectin (Mut 1) with key amino acid residue switches that are expected to make the L-selectin behave more P-selectin-like, against PSGL-1 or other PSGL-1-derived glycosulfopeptides. The key switches in the amino acids are in the lectin domain of L-selectin. Consistent with these observations, when Mut 1 was tested against 2-GSP-6, the results were dramatically different from the wild type L-selectin data (Yago et al., unpublished data). For wild type L-selectin, the *Off-rate vs. Force* curve was biphasic with a catch-slip transitional bond. On the contrary, for the Mut 1 data, the off-rates were consistently smaller than those of the wild type at low force regime (meaning stronger or more P-selectin-like interactions). Also, it was marked by a conspicuous absence of catch-slip transitional bonds, with the off-rate increasing exponentially with force (slip bond behavior). This has also been confirmed by corresponding rolling velocity measurements and analyses and AFM experiments in our lab (Yago et al., unpublished data). The amino acid(s) switch was designed in a way such that only interactions with PSGL-1 (or any other PSGL-1-derived glycosulfopeptides) and not 6-sulfo-sLe^x, a key recognition determinant of O-glycans on lymph node vessels would be affected. Consistent with the design, neither the *Off-rate vs. Force* nor the rolling velocity data was different between wild type and Mut 1 L-selectin interacting with 6-sulfo-sLe^x. Again,

this has been independently confirmed by AFM experiments in our lab (Yago et al., unpublished data).

While the mutation is a static change (cause) that produces the abolishment of catch bonds (effect), it is very interesting to note that changing loading rate also causes very similar effect (*cf.* Figure 25 and 29). The effect of increasing loading rate, in essence mimics the effect of the residue substitution in the mutant L-selectin studies, though not on an equivalent note. Also, it should be noted that both residue switch and altering bond loading rate impacted L-selectin-sPSGL-1 (and -2-GSP-6) and not L-selectin-6-sulfo-sLe^x interactions. This offers some insight into the structural basis for the catch-slip transitional bond behavior. A key structural component in the peptide component of PSGL-1 (that is known to interact with the lectin domain of L-selectin) could be a key cause for the elimination of catch bonds by residue substitutions or increasing bond loading rates. Also, the sugar component of 6-sulfo-sLe^x could serve as another key component that is not affected by mutation or bond loading rate, when L-selectin interacts with it. This could imply that though L-selectin can interact with PSGL-1 (or PSGL-1-like ligands) as well as Peripheral Node Addressin, PNAd (or PNAd-like ligands), there could be different structural bases for these interactions, as is brought out by the mutation and loading rate studies. Exploring the structural bases for the catch-slip transitional bond behavior would be an area of interesting and exciting future work.

6.2.2 Rupture Force Experiments and DFS Analysis

The data discussed in specific aim # 3 were all obtained by using a ramp and hold assay (lifetime assay). It would be interesting to see how the bonds behave if they are subjected to a continuous ramp until rupture. The theory of DFS could then be employed

to test whether L-selectin interactions also show apparent discrepancies between lifetime and rupture force assays, just as P-selectin interactions did (i.e. before being analyzed on a common platform, namely the time-to-rupture analysis). If it can be shown that the apparent discrepancies (if any) in the L-selectin interactions can be satisfactorily addressed using the time-to-rupture analysis, this would serve as an independent proof of force history concept at work in L-selectin interactions as well. This would bolster the data already discussed in specific aim # 3 by a great extent.

CHAPTER 7

CONCLUSIONS AND FUTURE WORK

7.1 Implications of this Project Work

In this project, selectin interactions with a host of physiologically relevant ligands as well as selectin-specific mAbs were undertaken. Several key issues were taken up, relevant hypotheses formulated and experiments were designed to put these hypotheses to test. There are many pros coming out of this project. A few of them are listed below.

(1) Efficacy of our AFM set-up to characterize single bonds

(2) Ability to differentiate between unbinding of interacting molecular pairs and unfolding of individual protein globular domains

(3) Ability to discriminate between monomeric and dimeric interactions

(4) Ability to predict individual molecular lengths based on dead zone data

(5) Consistency of AFM results with independent Flow Chamber studies

(6) Demonstration of catch bonds in L-selectin-mediated interactions

(7) Demonstration of a novel force history dependence of forced L-selectin-ligand dissociation

(8) Possible insights into the structural bases of catch-slip transitional bond behavior

An insight into the mechanical features of the selectins and how they were able to withstand very high strains without any catastrophic unfolding of their protein globular domains in the AFM experiments could provide a potential reason as to why these

molecules are so efficient in capturing leukocytes under flow conditions. At this juncture, no palpable link seems to exist between the mechanical properties of the selectins and their kinetic properties. Fritz et al. were the first ones to publish elasticity numbers for P-selectin-PSGL-1 complex (Fritz et al. 1998). In this project, we have adopted a systematic and detailed approach to probe the mechanical properties of selectin-ligand bonds.

Till recently, catch bonds existed only as a theoretical possibility (Dembo et al. 1988) and were only recently demonstrated in P-selectin-ligand interactions (Marshall et al. 2003). At that point, it was thought that catch bonds could be a causal factor for the shear threshold effect observed in selectin-mediated interactions. In this study, we have demonstrated that L-selectin-mediated interactions also exhibit catch bonds and that catch bonds could be an inherent property of selectin-mediated interactions. The one-to-one relationship between catch bonds and shear threshold has been satisfactorily explained in a very recent study (Yago et al. 2004), thus offering the very first biological relevance of catch bonds.

The concept of force history is relatively new-fangled and it challenges an existing paradigm that has been accepted by many. This concept provides us with a new paradigm of how force can regulate biological interactions at the single molecular level. Also, the fact that changing a physical parameter (bond loading rate) would induce the same change as a mutation is very insightful in terms of identifying the structural bases for catch-slip transitional bonds. Biophysical studies like these would serve as a bridge between engineering and traditional biology.

Dynamic models of selectin-ligand interactions could be used for the design and development of selectin-based anti-inflammatory drugs. In this regard, this project assumes significance. Hopefully, data obtained from this project would not only add to the existing body of knowledge but also help us in the process of identifying key mechanisms by which selectins initiate leukocyte adhesion under shear.

7.2 Pitfalls of this Project Work

In this project, AFM was used to characterize molecular properties devoid of cellular properties. Predictions about the biological implications based on the AFM studies alone could be tricky as the same pair of interacting molecules would behave differently on the surface of a cell. This is because the cell is a dynamic and living entity, being constantly bombarded by signals from outside and inside. How the molecules behave when they are expressed on cell surfaces would be dependent heavily on the biochemical signals they receive. Hence, it would not be wise to extrapolate any AFM findings to cellular behavior without carrying out similar but independent studies using other assays like Flow Chamber, which could use live cells, as against purified molecules.

The AFM used for this project was built and calibrated in-house in our lab. This AFM is equipped with a Piezo that could be actuated in the z-direction only. Having a Piezo that can be actuated along all three directions would be a valuable addition to the system. This would enable one to carry out on-rate and off-rate studies as a function of the distance between apposing molecular pairs.

7.3 Future Work

The most exciting thing about research is that it breeds more research. As such, there could never be an end to the plethora of questions and issues that could be pursued. While it is good to identify key issues, care should be taken to look into the biological relevance of the issues being pursued. With this in mind, a few directions for future studies can be identified.

7.3.1 Establishment of a Direct Relationship between Shear Threshold and Catch Bonds

Flow chamber experiments have revealed a counter-intuitive threshold requirement for selectin-mediated leukocyte rolling: as shear drops below the threshold, rolling becomes unstable and faster, and cells detach from the endothelia (Finger et al. 1996). It has been shown that mild metaperiodate oxidation of the carbohydrate moieties abolishes the shear threshold in L-selectin-mediated cell rolling (Puri and Springer 1996). It would be interesting to check whether catch bonds are abolished when metaperiodate-oxidized ligands interact with L-selectin, which will provide an independent demonstration of the relationship between catch bonds and shear threshold phenomenon.

7.3.2 On-rate Studies

Having an AFM with x-y and z Piezo actuators would be extremely useful to carry out on-rate studies as a function of molecular distance. To date, no comprehensive on-rate studies for the selectins have been carried out. Such a project would be an ideal start for more research in this direction. Also, varying the approach speeds of the AFM

cantilever and characterizing the binding can throw light on the association kinetics of these interactions.

7.3.3 AFM Studies with Other Super-Family CAMs

Currently, some members of the integrin family of CAMs are being actively studied in our lab, using AFM. The results though preliminary, are nonetheless very insightful. There are several qualitative ***and*** quantitative differences between selectin- and integrin-mediated interactions. Along similar lines, Fcγ receptor studies could be undertaken using AFM. Data pertaining to these receptors are readily available from literature and from our very own lab obtained using Confocal Microscopy (Tolentino et al., unpublished data). AFM studies could add an extra dimension to the existing body of data, by evaluating how force could regulate these interactions as well.

REFERENCES

Alon et al. (1998). "The kinetics and shear threshold of transient and rolling interactions of L-selectin with its ligand on leukocytes." *Proc Natl Acad Sci U S A* 95(20): 11631-11636.

Alon et al. (1997). "The kinetics of L-selectin tethers and the mechanics of selectin-mediated rolling." *J Cell Biol* 138(5): 1169-1180.

Alon et al. (1996). "Interactions through L-selectin between leukocytes and adherent leukocytes nucleate rolling adhesions on selectins and VCAM-1 in shear flow." *J Cell Biol* 135(3): 849-865.

Alon et al. (1995). "Lifetime of the P-selectin-carbohydrate bond and its response to tensile force in hydrodynamic flow." *Nature* 374(6522): 539-542.

Barkalow et al. (2000). "Dimerization of P-selectin in platelets and endothelial cells." *Blood* 96(9): 3070-7.

Bell, G. I. (1978). "Models for the specific adhesion of cells to cells." *Science* 200(4342): 618-627.

Binnig et al. (1986). "Atomic Force Microscope." *Phys. Rev. Lett.* 56: 930-933.

Chang and Hammer (1999). "The forward rate of binding of surface-tethered reactants: effect of relative motion between two surfaces." *Biophys J* 76(3): 1280-1292.

Chang et al. (2000). "The state diagram for cell adhesion under flow: leukocyte rolling and firm adhesion." *Proc Natl Acad Sci U S A* 97(21): 11262-11267.

Chen and Springer (1999). "An automatic braking system that stabilizes leukocyte rolling by an increase in selectin bond number with shear." *J Cell Biol* 144(1): 185-200.

Dammer et al. (1996). "Specific antigen/antibody interactions measured by atomic force microscopy." *Biophys. J.* 70(May): 2437-2441.

Dembo et al. (1988). "The reaction-limited kinetics of membrane-to-surface adhesion and detachment." *Proc R Soc Lond B Biol Sci* 234(1274): 55-83.

Dustin et al. (1989). "Correlation of CD2 binding and functional properties of multimeric and monomeric lymphocyte function-associated antigen 3." *J Exp Med* 169(2): 503-517.

Epperson et al. (2000). "Noncovalent association of P-selectin glycoprotein ligand-1 and minimal determinants for binding to P-selectin." *J Biol Chem* 275(11): 7839-7853.

Evans, E. (1998). "Energy landscapes of biomolecular adhesion and receptor anchoring at interfaces explored with dynamic force spectroscopy." *Faraday Discuss* 111: 1-16.

Evans, E. (1999). "Looking inside molecular bonds at biological interfaces with dynamic force spectroscopy." *Biophys Chem* 82(2-3): 83-97.

Evans et al. (2004). "Mechanical switching and coupling between two dissociation pathways in a P-selectin adhesion bond." *Proc Natl Acad Sci U S A* 101(31): 11281-11286.

Evans et al. (2001). "Chemically distinct transition states govern rapid dissociation of single L-selectin bonds under force." *Proc. Natl. Acad. Sci. USA* 98: 3784-3789.

Evans, E. and K. Ritchie (1997). "Dynamic strength of molecular adhesion bonds." *Biophys J* 72(4): 1541-1555.

Fieger et al. (2003). "Endoglycan, a member of the CD34 family, functions as an L-selectin ligand through modification with tyrosine sulfation and sialyl Lewis x." J *Biol Chem* 278(30): 27390-27398.

Finger et al. (1996). "Adhesion through L-selectin requires a threshold hydrodynamic shear." *Nature* 379(6562): 266-269.

Florin et al. (1994). "Adhesion forces between individual ligand-receptor pairs." *Science* 264: 5157.

Fritz et al. (1998). "Force-mediated kinetics of single P-selectin/ligand complexes observed by atomic force microscopy." *Proc Natl Acad Sci U S A* 95(21): 12283-12288.

Geng et al. (1990). "Rapid neutrophil adhesion to activated endothelium mediated by GMP-140." *Nature* 343(6260): 757-760.

Hutter, J. L. and J. Bechhoefer (1993). "Calibration of atomic-force microscope tips." *Rev Sci Instrum* 64: 1868-1873.

Johnston et al. (1989). "Cloning of GMP-140, a granule membrane protein of platelets and endothelium: sequence similarity to proteins involved in cell adhesion and inflammation." *Cell* 56(6): 1033-1044.

Kellermayer et al. (1997). "Folding-unfolding transitions in single titin molecules characterized with laser tweezers." *Science* 276(5315): 1112-1116.

Kishimoto et al. (1990). "Identification of a human peripheral lymph node homing receptor: a rapidly down-regulated adhesion molecule." *Proc Natl Acad Sci U S A* 87(6): 2244-2248.

Lawrence, M. B. (1999). "Selectin-carbohydrate interactions in shear flow." *Curr Opin Chem Biol* 3(6): 659-664.

Lawrence et al. (1997). "Threshold levels of fluid shear promote leukocyte adhesion through selectins (CD62L,P,E)." *J Cell Biol* 136(3): 717-727.

Li et al. (1998). "Regulation of L-selectin-mediated rolling through receptor dimerization." *J Exp Med* 188(7): 1385-1390.

Marshall et al. (2003). "Direct observation of catch bonds involving cell-adhesion molecules." *Nature* 423(6936): 190-193.

Marshall et al. (2004). "Force History Dependence of Receptor-Ligand Dissociation." *Biophys J.* 88:1458-1466.

McConnell et al. (1986). "Supported planar membranes in studies of cell-cell recognition in the immune system." *Biochim Biophys Acta* 864(1): 95-106.

McEver, R. P. (1990). "Properties of GMP-140, an inducible granule membrane protein of platelets and endothelium." *Blood* 16(1): 73-80.

McEver, R. P. (1991). "Leukocyte interactions mediated by selectins." *Thromb Haemost* 66(1): 80-87.

McEver, R. P. (1991). "Selectins: novel receptors that mediate leukocyte adhesion during inflammation." *Thromb Haemost* 65(3): 223-228.

McEver, R. P. (1994). "Selectins." *Curr Opin Immunol* 6(1): 75-84.

McEver, R. P. (2002). "Selectins: lectins that initiate cell adhesion under flow." *Curr Opin Cell Biol* 14(5): 581-586.

McEver, R. P. (2004). "Interactions of selectins with PSGL-1 and other ligands." *Ernst Schering Res Found Workshop*(44): 137-147.

McEver, R. P. and R. D. Cummings (1997). "Role of PSGL-1 binding to selectins in leukocyte recruitment." *J Clin Invest* 100: 97-103.

Merkel et al. (1999). "Energy landscapes of receptor-ligand bonds explored with dynamic force spectroscopy." *Nature* 397(6714): 50-53.

Moore et al. (1995). "P-selectin glycoprotein ligand-1 mediates rolling of human neutrophils on P-selectin." *J Cell Biol* 128(4): 661-671.

Moore et al. (1992). "Identification of a specific glycoprotein ligand for P-selectin (CD62) on myeloid cells." *J Cell Biol* 118(2): 445-456.

Perret et al. (2004). "Trans-bonded pairs of E-cadherin exhibit a remarkable hierarchy of mechanical strengths." *Proc Natl Acad Sci U S A* 101(47): 16472-16477.

Puri, K. D. and T. A. Springer (1996). "A schiff base with mildly oxidized carbohydrate ligands stabilizes L-selectin and not P-selectin or E-selectin rolling adhesions in shear flow." *J Biol Chem* 271(10): 5404-5413.

Ramachandran et al. (1999). "Tyrosine replacement in P-selectin glycoprotein ligand-1 affects distinct kinetic and mechanical properties of bonds with P- and L-selectin." *Proc Natl Acad Sci U S A* 96(24): 13771-13776.

Ramachandran et al. (2001). "Dimerization of a selectin and its ligand stabilizes cell rolling and enhances tether strength in shear flow." *Proc Natl Acad Sci U S A* 98(18): 10166-10171.

Rief et al. (2000). "Unfolding forces of titin and fibronectin domains directly measured by AFM." *Adv Exp Med Biol* 481: 129-36; discussion 137-141.

Rief et al. (1997). "Reversible unfolding of individual titin immunoglobulin domains by AFM." *Science* 276(5315): 1109-1112.

Rief et al. (1998). "The mechanical stability of immunoglobulin and fibronectin III domains in the muscle protein titin measured by atomic force microscopy." *Biophys J* 75(6): 3008-3014.

Salinas, P. C. and S. R. Price (2005). "Cadherins and catenins in synapse development." *Curr Opin Neurobiol* 15(1): 73-80.

Sarangapani et al. (2004). "Low force decelerates L-selectin dissociation from P-selectin glycoprotein ligand-1 and endoglycan." *J Biol Chem* 279(3): 2291-2298.

Shao et al. (1998). "Static and dynamic lengths of neutrophil microvilli." *Proc Natl Acad Sci U S A* 95(12): 6797-6802.

Shimaoka et al. (2000). Computational design of an integrin I domain stabilized in the open, high affinity conformation. *Nature Struct. Biol.*7:674-678.

Snapp et al. (1998). "A novel P-selectin glycoprotein ligand-1 monoclonal antibody recognizes an epitope within the tyrosine sulfate motif of human PSGL-1 and blocks recognition of both P- and L-selectin." *Blood* 91(1): 154-164.

Springer, T. A. (1985). "The LFA-1, Mac-1 glycoprotein family and its deficiency in an inherited disease." *Fed Proc* 44(10): 2660-2663.

Springer, T. A. (1990). "Adhesion receptors of the immune system." *Nature* 346(6283): 425-434.

Springer, T. A. (1990). "The sensation and regulation of interactions with the extracellular environment: the cell biology of lymphocyte adhesion receptors." *Annu Rev Cell Biol* 6: 359-402.

Springer, T. A. (1994). "Traffic signals for lymphocyte recirculation and leukocyte emigration: the multistep paradigm." *Cell* 76(2): 301-314.

Ushiyama et al. (1993). "Structural and functional characterization of monomeric soluble P-selectin and comparison with membrane P-selectin." *J Biol Chem* 268(20): 15229-15237.

Wong et al. (1999). "Polymer-cushioned bilayers. I. A structural study of various preparation methods using neutron reflectometry." *Biophys J* 77(3): 1445-1457.

Wong et al. (1999). "Polymer-cushioned bilayers. II. An investigation of interaction forces and fusion using the surface forces apparatus." *Biophys J* 77(3): 1458-1468.

Yago et al. (2002). "Distinct molecular and cellular contributions to stabilizing selectin-mediated rolling under flow." *J Cell Biol* 158(4): 787-799.

Yago et al. (2004). "Catch bonds govern adhesion through L-selectin at threshold shear." *J Cell Biol* 166(6): 913-923.

Zhao et al. (2001). "Dynamic contact forces on leukocyte microvilli and their penetration of the endothelial glycocalyx." *Biophys J* 80(3): 1124-1140.

Zhurkov, S. N. (1965). "Kinetic Concept of the Strength of Solids." *Int. J. Fracture Mech.* 1: 311-322.

VITA

Krishna Kumar Sarangapani did his UG education in India and joined the Masters program in Environmental Engineering at The Georgia Institute of Technology, Atlanta, GA in Fall 2000. He shifted to the Bioengineering PhD program in Spring 2001 and under the guidance of Dr. Cheng Zhu, completed his degree in Summer 2005.

EDUCATION

PhD in Bioengineering
Georgia Institute of Technology, Atlanta, Georgia
Graduation Date: Summer 2005

Bachelor of Technology (Honors) in Biotechnology and Biochemical Engineering
Indian Institute of Technology (IIT), Kharagpur, India
Graduation Date: Summer 2000

HONORS AND AWARDS

- Second Place in the Student Paper Competition in ASME 2005 Summer Bioengineering Conference held in Vail, CO
- Recipient of the 2004 Suddath Award for outstanding Doctoral Research (Awarded to the Best Predoctoral Graduate Student within the Departments of Biology, Chemistry & Biochemistry and Biomedical Engineering)
- Recipient of the Student Paper Competition Award in BMES 2003 Conference held in Nashville, TN
- Completed Undergraduate Program in IIT with First Rank in Class
- Top 1% of ~ 200,000 candidates in the National Level Entrance Exam for the IITs

JOURNAL PUBLICATIONS

- **K. K. Sarangapani**, T. Yago, A. G. Klopocki, M. B. Lawrence, C. B. Fieger, S. D. Rosen, R. P. McEver and C. Zhu. Low Force decelerates L-selectin

dissociation from P-selectin Glycoprotein Ligand 1 and Endoglycan. (2004) *J. Biol. Chem.,* 279:2291-2298

- B. T. Marshall, **K. K. Sarangapani**, J. Lou, R. P. McEver and C. Zhu. Force History Dependence of Receptor-Ligand Dissociation. (2005) *Biophys. J.,* 88: 1458:1466

- **K. K. Sarangapani**, B. T. Marshall, J. Wu, R. P. McEver and C. Zhu. Measuring Molecular Elasticity by Atomic Force Microscope Cantilever Fluctuations. *Biophys. J.* (Manuscript in Preparation)

- **K. K. Sarangapani**, B.T. Marshall, M. B. Lawrence, R. D. Cummings, R. P. McEver and C. Zhu. Molecular Elasticity of Selectins (Manuscript in Preparation)

- **K. K. Sarangapani**, M. B. Lawrence, R. D. Cummings, R. P. McEver and C. Zhu. Direct Observation of Force History Dependence of Lifetimes of L-selectin-Ligand Bonds (Manuscript in Preparation)

CONFERENCE PUBLICATIONS

- **K. K. Sarangapani**, B. T. Marshall, R. P. McEver and C. Zhu. Dead Zone Distributions in Selectin-Mediated Interactions. ASME Summer Bioengineering Conference, June 22-26, 2005, Vail, CO

- **K. K. Sarangapani**, B. T. Marshall, J. Wu, M. B. Lawrence, R. P. McEver and C. Zhu. Probing Single Molecule Interactions using Atomic Force Microscopy. BMES Annual Fall Meeting, October 13-16, 2004, Philadelphia, PA

- **K. K. Sarangapani**, M. B. Lawrence, R. P. McEver and C. Zhu. Molecular Elasticity of the Selectins. BMES Annual Fall Meeting, October 1-4, 2003, Nashville, TN

- **K. K. Sarangapani**, M. B. Lawrence, R. P. McEver and C. Zhu. Characterizing L-selectin-PSGL-1 interactions using Atomic Force Microscopy. Second Joint Meeting of BMES and IEEE-EMBS, October 22-26, 2002, Houston, TX

- N. Jiang, **K. K. Sarangapani**, P. Selvaraj and C. Zhu. Measuring Kinetics of Fcγ Receptor III (CD16) binding to Human IgG1 in real-time using Flow Cytometry. BMES Annual Fall Meeting, October 4-7, 2001, Durham, NC